Structural Assessment of Difficult Pipeline at Bends

By

Azrulfirdaus bin Muhamad Roshdi

Dissertation submitted in partial fulfilment of
The requirement for the
Bachelor of Engineering (Hons)
(Civil Engineering)

SEPTEMBER 2013

Universiti Teknologi PETRONAS
Bandar Seri Iskandar
31750 Tronoh
Perak Darul Ridzuan
Malaysia

CERTIFICATION OF APPROVAL

Structural Assessment of Difficult Pipeline at Bends

By

Azrulfirdaus bin Muhamad Roshdi

A project dissertation submitted to the
Civil Engineering Programme
Universiti Teknologi PETRONAS
In partial fulfilment of the requirement for the
BACHEOR OF ENGINEERING (Hons)
(CIVIL ENGINEERING)

Approved by,

____

(Dr. Zahiraniza Binti Mustaffa)

UNIVERSITI TEKNOLOGI PETRONAS
TRONOH, PERAK
SEPTEMBER 2013

CERTIFICATION OF ORIGINALITY

This is to certify that I am responsible for the work submitted in this project, that the original work is my own except as specified in the references and acknowledgements, and that the original work contained herein have not been undertaken or done by unspecified sources or persons.

AZRULFIRDAUS BIN MUHAMAD ROSHDI

ABSTRACT

In a difficult pipeline, pipe bends are critical section that needs to be inspected for its reliability. The purpose of this research is to investigate the structural integrity of the difficult pipeline at bends. Finite Element Simulation method was used. Circular pitting corrosion at different depth and diameter were applied to simulate the stress distribution at three (3) different pipe models; standard 90° pipe bend, miter bend and unbarred full-bore tees pipe bend near dead end. The results of different corrosion equivalent stress, σ distribution were compared. At the end of this research, the finite element modelling (FEM) simulation was proven to be reliable for inspection of difficult pipeline at bends.

ACKNOWLEDGEMENTS

Praise to god, thank for all his blessing; most of all, I want to give thanks for His amazing love that knows no boundaries and endures forever. Through the experience of life, I have learnt and am still learning that I am strong when I am on his shoulders. I want to thank Him for all his wonderful thoughts of me and for raising me up to so much more than I can be.

I want to express my greatest gratitude to my supervisor, Dr. Zahiraniza Binti Mustaffa for her generosity, kindness and guidance throughout the project. It is not just the guidance that she gave, but she ensured that I got proper understanding and exercising to carry out my responsibilities. She did not reprimand me when I made mistakes, but was always gracious towards me. I can honestly say that I have benefited lots under her supervision.

Not to forget, special thanks to Dr Thar Albarody for helping me alongside Dr Zahiraniza in ensuring the completion of this project. Without his help and assistance, I am very sure that this project will just not be as it is for now.

Last but not least, my greatest appreciation goes to those who have assisted me directly or indirectly starting from the beginning of the project. Your utmost cooperation is highly appreciated and may God repay your kindness.

Thanks.

TABLE OF CONTENTS

LIST OF FIGURES

LIST OF TABLES

CHAPTER 1

INTRODUCTION

1.1. Project Background

At present, with the industry developed rapidly, the demand on the oil and gas is increasing hence the carrying ability and the transporting efficiency of pipeline has been improved. An accurate data and estimation on the pipeline condition is very important for its integrity assessment. In the design of the pipeline system, the use of pipe bend is important to cross obstacle and directional change of the flow.

Pipe bends are critical components in piping system. Pipe bends are curved bar with annular cross section whose reaction to external loading is complex. Therefore, the life assessment and failure prediction of pipe bends is an important factor to be considered in the design and safe operation of pipelines.

A typical in-line inspection tool is an ultrasonic tool which are especially suitable if there are high requirements regarding sensitivity and accuracy, which is especially relevant in offshore pipeline. This tools are also known as pig.

For a difficult pipelines, defines as pipelines that cannot be inspected by standard pigs, an entirely new direction in research and development has to be initiated. Various case of difficult pipeline can be found in a pipeline system, such as mitered bends, diameter reduction, dead ends and off takes.

Among this type of difficult pipelines, unbarred full-bore pipe bend near dead end is to be focus in this paper. This paper tends to analyse the effect of corrosion to the pipe bend by using finite element analysis. In this research, simulated corrosion was introduced to pipe bends to predict the integrity of the finite element model.

1.2. Problem Statement

The bend section may be potential source of damage during service. The pipelines can be subjected to combination of soil pressures, temperature variations and soil settlements. The variation of stresses in the longitudinal and the radial directions may lead to plasticity in combination of internal pressure.

Previous research works found out that numerical method analysis has become a reliable engineering approach towards achieving actual design pressure calculation. In this project, finite element analysis will be implemented to provide an allowable corrosion concentration at a pipe bend near dead end as illustrated in the figure 1.

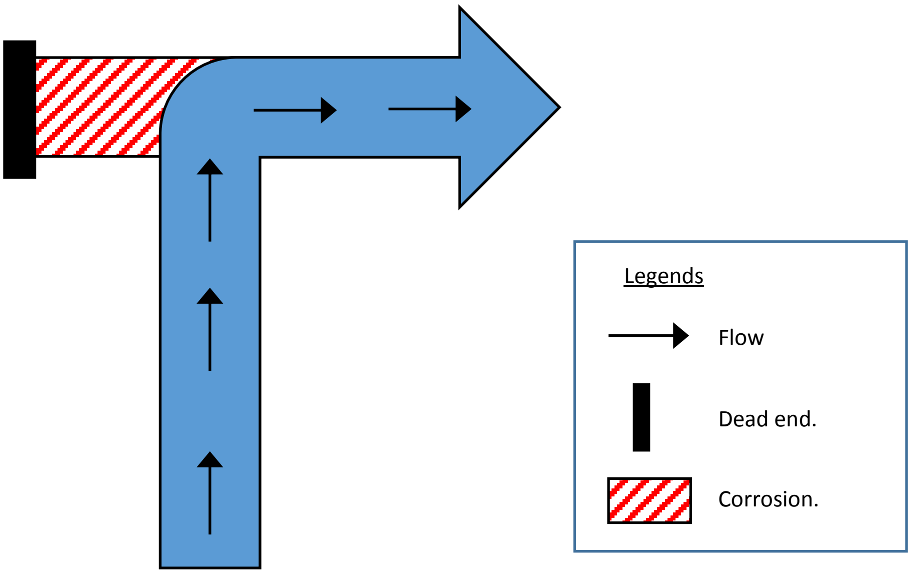

Figure 1: Corrosion at ignored areas due to unpiggability.

1.3. Scope of Study/Objective

The scope of this research is to assess the integrity of pipe bend using finite element modelling (FEM) method. The software that was used is the engineering simulation software, ANSYS. Precisely, the detailed scope of work for this simulation are as follow:

a. Identify and characterise the standard pipe bend, miter bend and unbarred full-bore pipe bend near dead end.
b. Provide model for standard pipe bend, miter bend and unbarred full-bore pipe bend near dead end.
c. Implement finite element analysis to the models.
d. Simulation of corrosion in the finite element models.
e. Analytically compare the result of the simulated models

Thus, this research intends to focus on the following objectives:

a. To develop a finite element model of standard pipe bend, miter bend and bend pipe near dead end.
b. To simulate stress distribution of the models under different corrosion depth.
c. To simulate stress distribution of the models at different area of corrosion.
d. To compare the maximum stress distribution at the models due to the applied corrosion.

1.4. Relevancy of Research

The finite element modelling is a powerful method to detect the failure zone of a model. The analyses provided in this paper carried out by using the commercial Finite element program ANSYS. The ANSYS Workbench 14.0 enables user to develop modelling and to carry out analyses. An effective use of computer resources is possible by the application of this useful instrument. All required data are written into files during each analysis and can be depicted graphically immediately afterwards.

1.5. Feasibility of Research

Based on the scope of work and time frame, this research is feasible. A lot of software simulation and documentation will be carried out. For software simulation, ANSYS was used. This software was provided by the university in the software lab. Hence, before the end of this period, the research would be completed.

CHAPTER 2

LITERATURE REVIEW

2.1. Introduction

Finite element analysis for corrosion at pipeline bend is a sample of unpiggability. Studies have proven that the result of finite element method is reliable for the pipeline integrity. Hence, this research will focused on the finite element simulation due to internal pressure to the pipeline bend.

2.2. Pigging

Pigging is a method used by pipeline engineer for operation and maintenance in pipeline business. A general definition of pigging is the propulsion through a pipe of a mobile plug pig which can be execute certain activities inside the pipe (Hiltscher, 2003). There are various use of pigging in pipeline such as to clean a pipe mechanically, to check a channel, or to inspect the welding seams of a pipeline. Hiltscher (2003) in their book listed the detailed field application of this pipeline pigging which are:

- Sweeping liquid from pipelines.
- Removing incrustation and deposits.
- Removing condensate.
- Filling/emptying of a pipeline by a flow plug.
- Separation of products pumped. This process is known as batch pigging.
- Inspection, detecting and observation.
- Cleaning.
- Measurement and control.
- Repairing.

Physically, the pig can be spherical, elongated or composed of several parts. Table 1 provide a general type of pigs with their respective advantages and limitation.

Table 1: Type of pigs

Name	Advantages	Limitations
Mandrel pig  Figure 2: Mandrel Pigs (“About Pigs”, 2013).	- Long-term, long-life. - Cups and discs easily replaceable. - Various brush types can be utilized for cleaning purpose.	- High redressing cost. - Larger pig require special handling equipment for loading and unloading. - Smaller size pigs will not negotiate 1.5D (D is diameter of pipe) bends.
Foam pig  Figure 3: Foam Pigs (“About Pigs”, 2013)	- Inexpensive and versatile. - Lightweight and flexible. - Compressible and expandable. - Can do various type of pipe, valve, fitting and bends.	- One-time use. - Short length of runs. - High acid concentration.
Solid cast pigs  Figure 4: Solid Cast Pigs (“About Pigs”, 2013)	- Maneuver in less than 1.5D radius ells and bends. - Add brush for cleaning purpose. - Hollow core adds flexibility.	- Wearing components cannot be replaced.
Smart pig  Figure 5: Smart Pig (“About Pigs”, 2013)	- Equipped with sensors. - Provide data such as dents, wrinkles, ovality, bend radius and angle, and corrosion indications	-

Spherical pigs  Figure 6: SmartTrap Automated Combo Pigging System *(Payne, 2012)*	- Magazine loaded by special launcher. - Negotiate short radius 90’s, irregular turns and bends - Able to go from small lateral line to larger main lines	- Cannot run in pipeline that have not flow trees installed
Plugs  Figure 7: Plugs (“About Pigs”, 2013)	- Withstand high pressure up to 200 bars	-
Gel pigs  Figure 8: Gel Pigs (“About pigs”, 2013)	- Do not wear out in service like conventional pigs - Can be pumped into any lines. - Used alone, in place of batching pigs or other conventional pigs	- Likely to be diluted - Susceptible to gas cutting

2.3. Smart Pigs

Pigs which not only consists of mechanical components (mechanical pigs), but also have an electrical/electronic part for measuring, processing, storing and transmitting data are termed smart pigs (Hiltscher, 2003). These pigs are used for in-line inspection of pipelines by the method of non-destructive testing of materials or optical inspection. In smart pigs, the following method of non-destructive testing are used:

- Magnetic Flux Leakage
- Ultra sonic
- Eddy current.

In magnetic flux leakage testing, a special brush magnet induce a magnetic field in the pipe wall. If the intensify of the magnetic field passing through the wall higher, it is a defected area.

During the transaction from one medium to another in ultrasonic testing, the larger the difference between the acoustic independence of the two media, the stronger is the sound reflected at the interface. Therefore air film between ultra sound generator and pipe wall must be displaced by oil or water.

Eddy current sensors can be made small and are easily built. They are therefore more suitable for the inspection of smaller pipelines (Hiltscher, 2003).

Still, many pipelines cannot be inspected, even with these enhanced technologies. These pipeline are known as unpiggable pipelines.

2.4. Difficult Pipelines

A pig is classified as unpiggable based on the following criteria (Krieg, 2013):

- No access, in case where the launcher and receiver are not equipped to the system.
- Existing piping component, such as 90° miter bends, dead ends, off-takes, reduction, dead end, one-cut bend, unbarred full bore T and valve.
- Flow at which is low or unavailable.
- Cleanliness of the pipe.

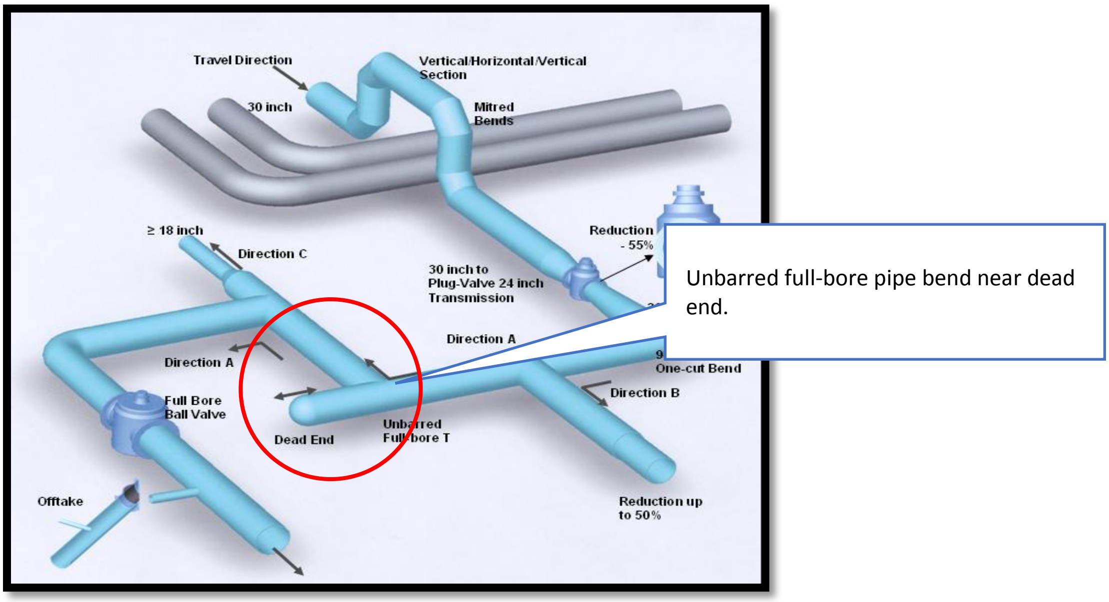

Figure 9: Unpiggable installation *(Krieg, 2013)*.

Fig. 9 shows the complete illustration of unpiggable installation in any pipeline system. In this research, only bend will be considered, particularly highlighted in circled red.

2.5. Pipe Bend

Wint (2013) categorised pipeline bend into two parts which are:

1) Mitered bends.
2) Common factory bends.

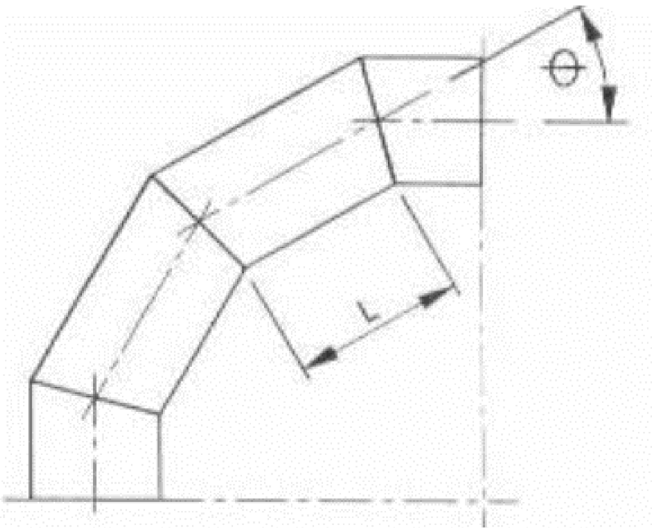

Figure 10: Typical Mitered Pipe Bend *(Wint, 2013)*

Fig. 10 shows the typical miter bend which is a bend that made up of cutting pipe end and connected to other pipe end at an angle.

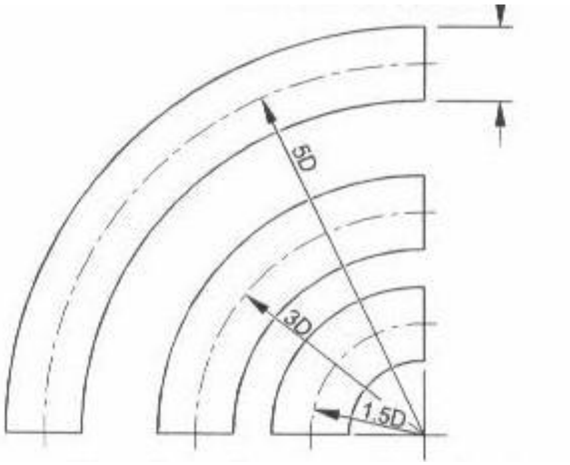

Figure 11: Common Factory Bends *(Wint, 2013)*

Based on fig 11, Wint (2013) described common factory bends are pipe with bend of 1.5D, 3D and 5D (D is diameter of pipe). Bends is also based on centreline radius (CLR) (Close Radius Pipe Bending, 2013). A pipe bend is classified according to the centreline radius (CLR) of the bend as a ratio to the nominal pipe diameter. For example, a 3D bend has its radius which is three times it nominal pipe diameter.

2.6. Finite Element Analysis on Pipe Bends

Kim et al. (2009) focused their research work on corrosion defect for hot bend pipe. Hot bend pipe is used for route change that is more than 16°. Magnitude of pre-strain and deformation is quantified for the finite element analysis. The burst pressure of the pipe bend with corrosion defects is predicted by applying bend coefficient and average thickness to the corroded pressure (P_{corr}) expression of a straight pipe. Estimation using individual and average thickness of a finite element result for burst pressure at 90° bend pipe with corrosion defect unsymmetrical/symmetrical position for extrados, crown and intrados was compared. Bhattacharya and Long (2010) investigated pipe bend for the stress intensification factor and flexibility factor. In the analysis, both within and outside the limitation of ASME B31 piping codes were tested. The result is then compared to the nominal stress of the pipe. Swart et al. (2010) used a numerical formulation in the analysis of the pipe bends. Gurson plasticity model simulated pipe behaviour due to the longitudinal deformation, ovalization and warping. Results were compared to selective integrated Heterosis elements. Eckart (1996) showed the bend loading capacity and fatigue strength based on finite element analyses of a pipe bend. It is proven that finite element analysis suits for the design of a pipe bend for fatigue strength and load carrying capacity. Among others, Prasad and Rao (2013) discussed the effect of applying internal pressure to the ovality of the bends. The result was summarised in the form of total deflection and stresses to the pipe bends.

Table 2 shows the summary of literature review that was completed up to the time of writing.

Table 2: Summary of literature review

No	Author	Title	Methodology	Result
1	Woosik Kim, Jonghyun Baek and Youngpyo Kim	Integrity assessment for corrosion defect in hot bend pipe of natural gas pipeline	The burst pressure of the pipe bend with corrosion defects is predicted by applying bend coefficient and average thickness to the corroded pressure of straight pipe	Magnitude of pre-strain and deformation in pipe bend
2	Anindya Bhattacharya and Daniel Long	A finite element-based investigation on stress intensification and flexibility factor for pipe bends within and outside the limitation of ASME B31 piping codes.	Pipe bend was investigated for the stress intensification factor and flexibility factor	Both within and outside the limitation of ASME B31 piping codes were tested. The result is then compared to the nominal stress of the pipe
3	A.E. Swart, S.A. Karamanos, A. Scarpas	Finite element analysis of damage in pipeline bends	The stresses and micro-damage development in steel pipelines were analyzed by finite element model.	The maximum damage development with the tube elements is lower than with the shell elements.
4	Eckart Weib, Andreas Lietzmann, and Jurgen Rdolph	Linear and nonlinear finite-element analyses of pipe bends	The analyses of bend loading capacity and fatigue strength based on finite element of a pipe bend	Finite element method proven to suit the loading capacity and fatigue strength.
5	Kaviti. R Vara Prasad and Tippa Bhimasankara Rao	Ovality in pipe bends by finite element analysis	Internal pressure applied to the ovality of the bends	The result is summarised in the form of total deflection and stresses to the pipe bends.

CHAPTER 3

METHODOLOGY

3.1. Pipeline Stresses and Load Identification

At early stage, stresses and loads need to be identified as they influence the failure prediction of a corroded pipeline. Internal pressure, axial and/or bending loads may need to be considered. The classification of the pressure loading are important in this research. For this research only the case of internal pressure loading was considered.

3.2. Corroded Pipeline Modelling using Finite Element Modelling (FEM)

Corroded pipelines modelled using finite element modelling (FEM) allow wide range of analysis. The FEM often involves various shapes of model and various material behaviour. The ANSYS® Workbench™ version 14.0 allows the user to simulate the critical area (the area where it is expected to fail) and to simulate deforming surfaces. The multiphysic capabilities of ANSYS enable the user to improve user product development processes, reduce analysis time, and improve product innovations and performances.

Modelling of corroded pipeline involves few stages before the analysis can be done. The stages consist of assigning pipe model properties, analysis system, modelling, meshing, defining loads and analysing results from solution. All of the stages mentioned are as follows:

3.2.1. Pipe model properties

For this research, three type of pipe was modelled. Standard 90° pipe bend, miter bend and tee near dead end.

All pipes were designed to match the recommended foam pig outer diameter as in the PTS 30.40.60.32. In this research, a foam pig with outside diameter of **450 mm** was selected.

In designing a miter bend, some extra calculation needed to be carry on to determine the nomenclature as stated in ASME B31.3. The following nomenclature is used for designing of a miter bend.

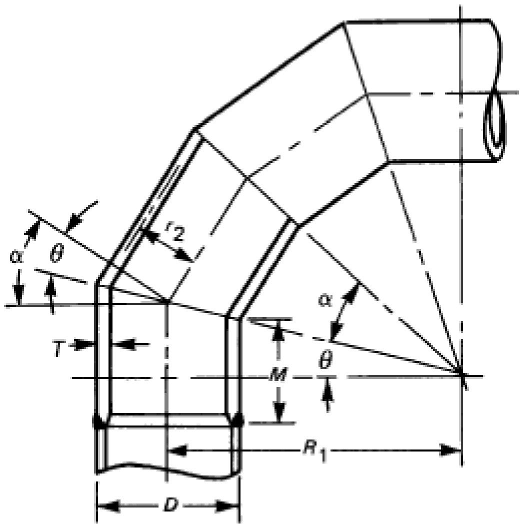

Figure 12: Nomenclature for miter bend.

r₂ = Mean radius of pipe using nominal wall
R₁ = Effective radius of miter bend
T = Miter pipe wall thickness
M = The larger of $2.5(r_2T)^{0.5}$ or $\tan\theta(R_1 - r_2)$
θ = Angle of miter cut
α = Angle of change in direction (2θ)

$$R_1 = \frac{A}{tan\,\theta} + \frac{D}{2}$$

Calculation of miter bend properties is shown in appendix.

Table 3 lists all pipe properties according to each code and standard.

Table 3: Pipe models properties

No	Pipe type	Code	Nominal Diameter, DN (mm)	Diameter, (cm)	Wall thickness, (cm)
1	Standard 90° pipe bend	PTS 31.38.01.11	450	45.72	1.745
2	Miter bend	ASME B31.3			
3	Unbarred full bored pipe bend near dead end.	ASTM A 234-WPB			

3.2.2. Analysis system

STATIC STRUCTURAL - A static structural analysis will be was used to determine the displacements, stresses, strains, and forces in structures or components caused by internal loading that do not induce significant inertia and damping effects. Steady loading and response conditions were assumed; that is, the loads and the structure's response are assumed to vary slowly with respect to time.

3.2.3. Modelling

All 3D models were generated by using **ANSYS**. The DesignModeler application is designed to be used as a geometry editor of existing CAD models. The DesignModeler application is a parametric feature-based solid modeller designed so that the users can intuitively and quickly begin drawing 2D sketches, modelling 3D parts, or uploading 3D CAD models for engineering analysis pre-processing.

The interface of DesignModeler is similar to other modellers. It contains toolbar, menus and all other solid modeller feature which user friendly and simple.

Fundamentally, this modeller allows the user to operate 2D sketching and 3D modelling.

In the sketching mode, there are five toolboxes to create 2D sketches by adding and removing 2D edges. From the 2D sketches, the user can generate 3D solid models. The modelling mode allows the users to create model by extruding, sweeping, revolving and generated primitive solid object.

For this research, three 3D models were created using the modeller.

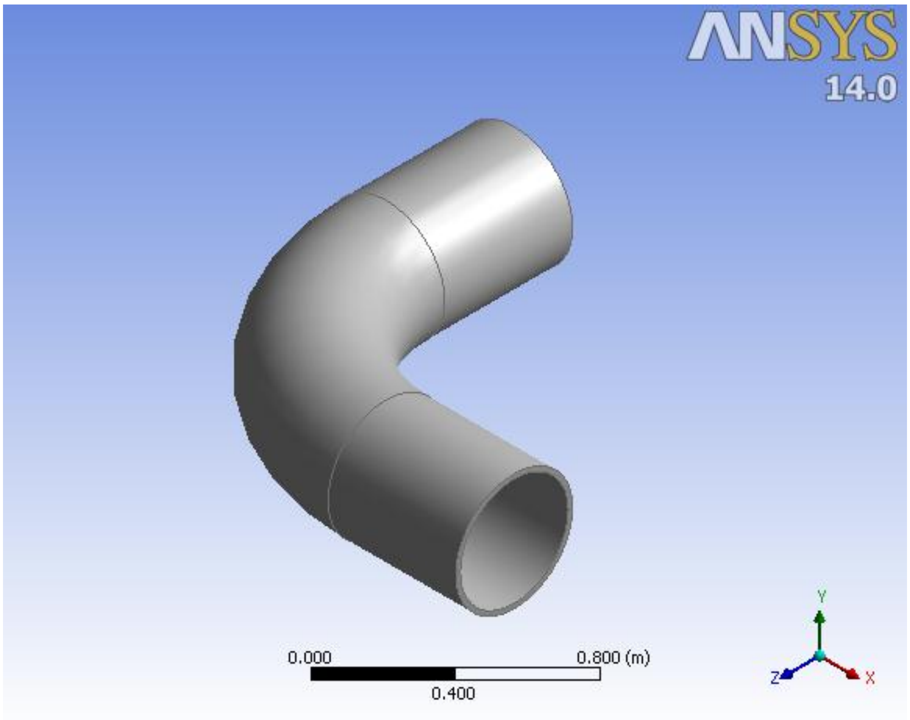

a. FEM sketch for standard 90° pipe bend

b. FEM sketch for miter bend

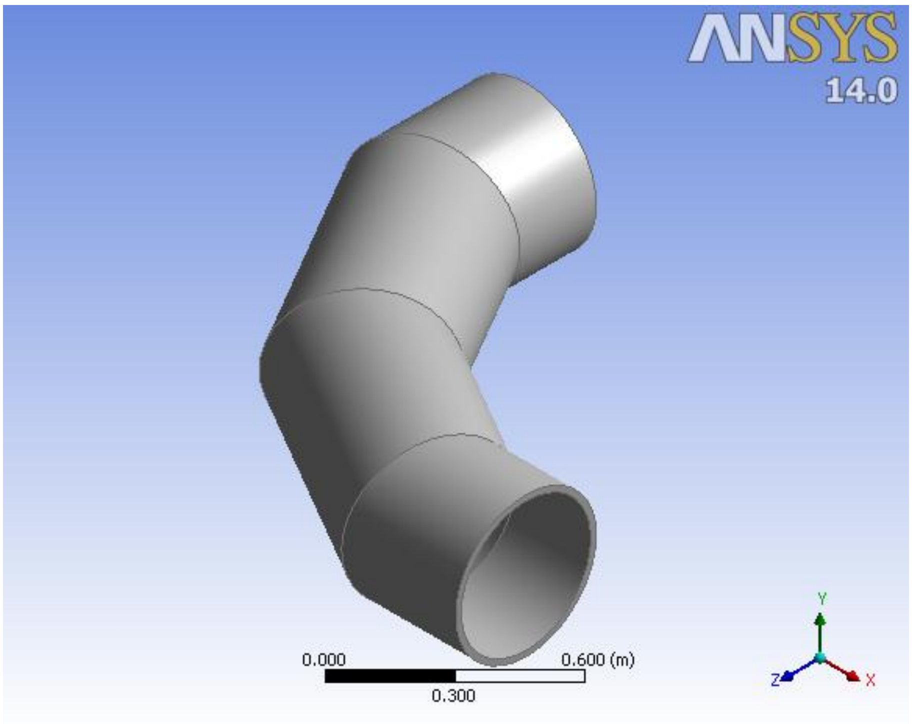

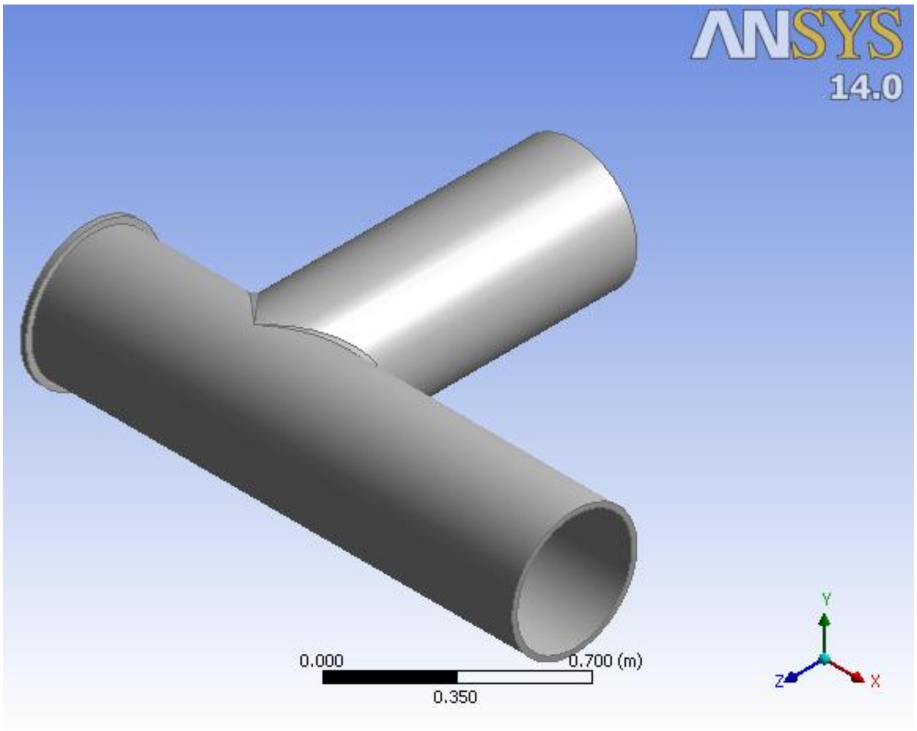

c. FEM sketch for unbarred full-bored pipe bend near dead end.

PITTING DEFECT MODELLING – pitting defect were defined as circular shape. It is defined as a volume taken out from the internal parts of the pipeline models. The modelling of the pitting is controlled by 2 dimensions which are the area of the pitting and depth of material cut.

a. Pitting corrosion inside a standard 90° pipe bend

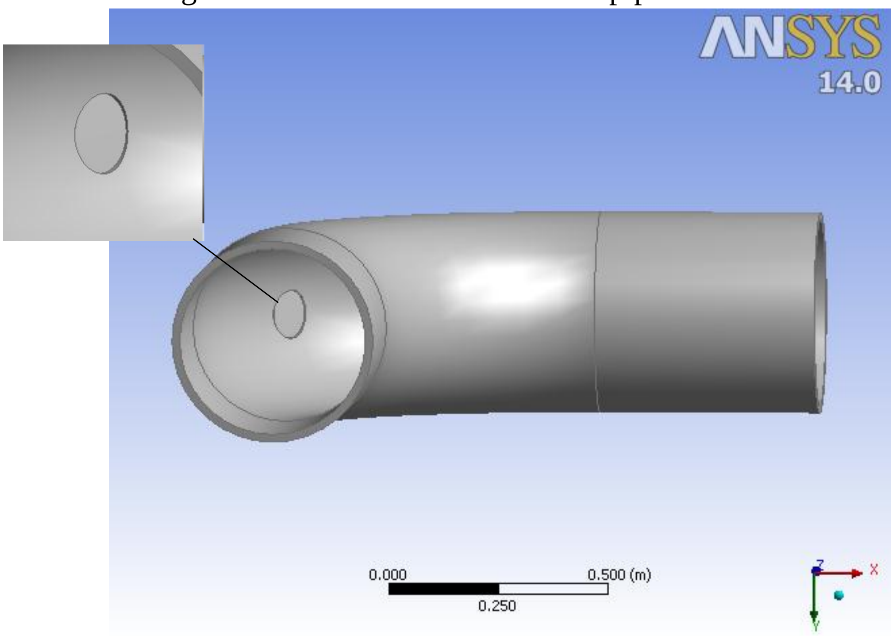

b. Pitting corrosion inside a miter bend

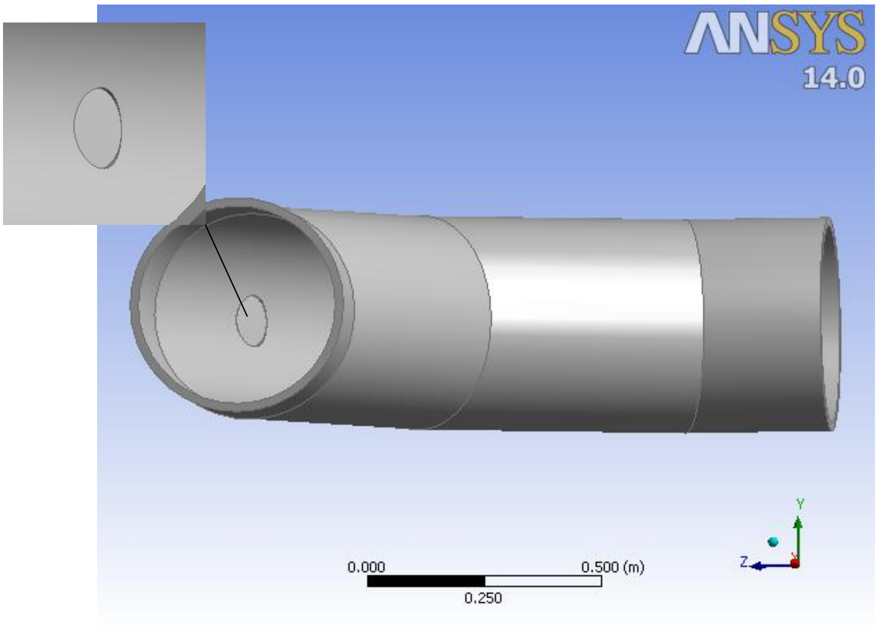

c. Pitting corrosion inside a tee pipe

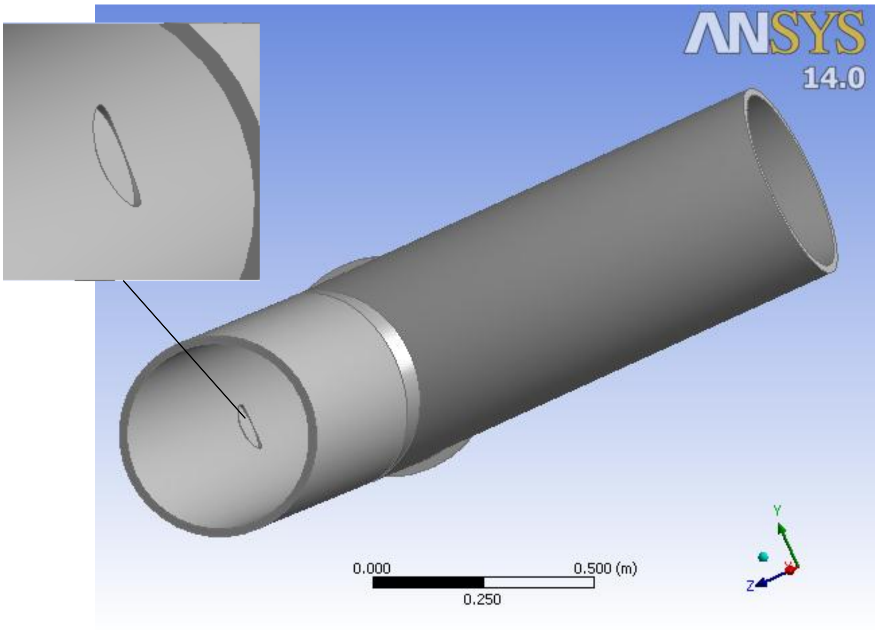

d. Pitting corrosion at an unpiggable area inside a tee pipe

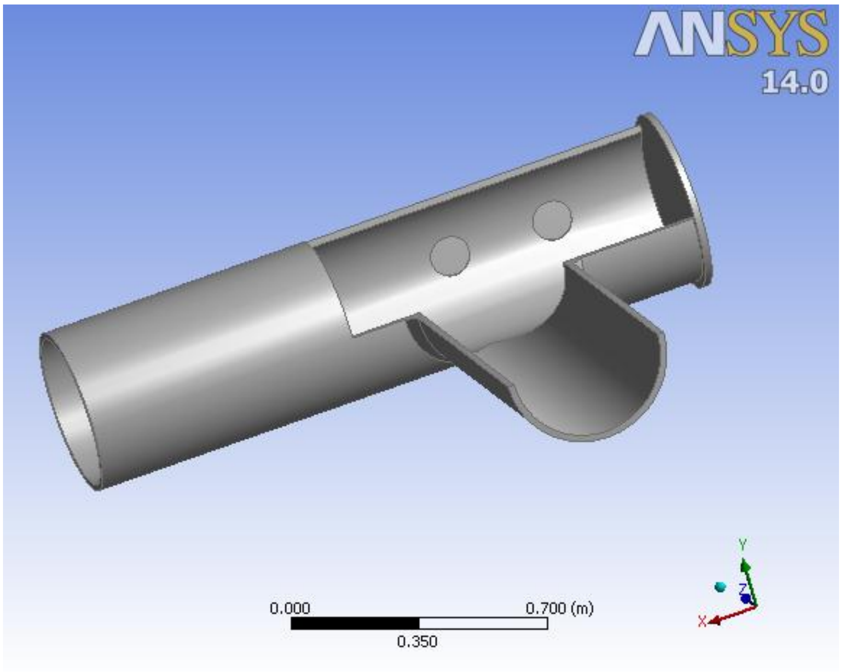

All these geometries were then used for meshing, load definition and analysing solution by using another ANSYS Workbench feature, **ANSYS® Mechanical™.**

3.2.4. Meshing

GENERAL MESHING – Meshing is one of the method used in FEM to run an analysis. Meshing represents field variable such as displacement polynomial function that produce a displacement field compatible with applied boundary condition. For the model in this project, element size sets to default settings so that it will be automatically generated and more practical for different corrosion area

3.2.5. Defining loads

STANDARD EARTH GRAVITY – Standard earth gravity (9.81 m/s^2) was applied to the models to add realistic environmental load to the pipe system. The followings are data regarding the load applied:

Table 4 : Standard earth gravity applied.

Object Name	*Standard Earth Gravity*
State	Fully Defined
Scope	
Geometry	All Bodies
Definition	
Coordinate System	Global Coordinate System
X Component	0. m/s²
Y Component	-9.8066 m/s²
Z Component	0. m/s²
Direction	-Y Direction

INTERNAL PRESSURE – The load was applied on the internal surface of the pipeline to represent the internal pressure subjected to pipeline. The magnitudes of load were manipulated in the ANSYS® Mechanical™ by setting the value of loading. The applied internal load was 250 bar.

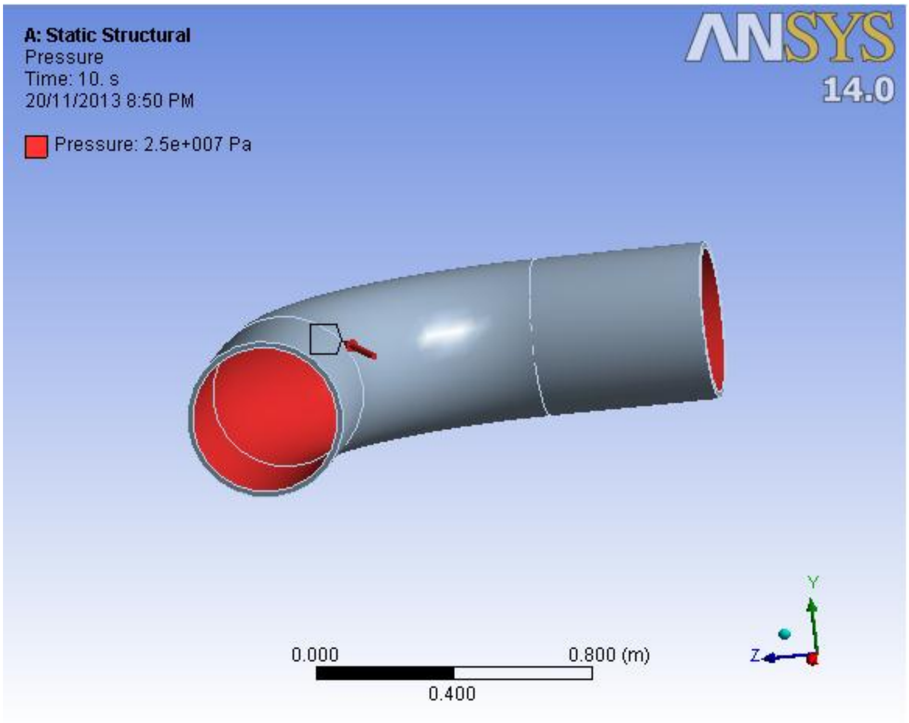

Figure 13: Applied internal pressure in a pipe bend

Fig. 13 shows internal pressure applied to the pipe bend in ANSYS® Mechanical™. The internal surface was red in colour to indicate it is under internal pressure in the analysis.

FIXED SUPPORT – Fixed support was applied at the edges of the pipe. It is to show the connection to other pipeline so that the model is fixed in moment, displacement, and shear at the edge.

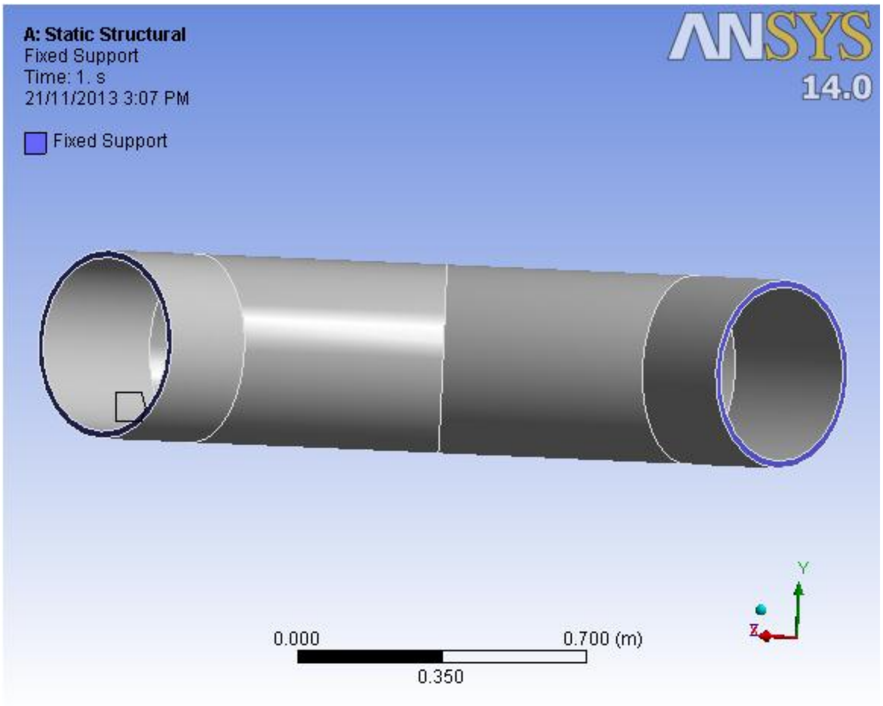

Figure 14 : Fixed support at Miter bend

Fig. 14 highlights the edge of miter bend at both ends due to fixed support. In the real case, both pipe ends are actually connected to other pipes.

3.2.6. Solution

TOTAL DEFORMATION – Total deformation solution needed to show the how the pipe bend deforms under internal pressure. Maximum total deformation from each model was recorded and compared to probe deformation (localised corrosion area) and to differentiate to other pipe models.

EQUIVALENT VON-MISES ELASTIC STRAIN/STRESS – The von Mises or equivalent strain, ε_e is computed as:

$$\varepsilon_e = \frac{1}{1+v'}\left(\frac{1}{2}[(\varepsilon_1-\varepsilon_2)^2+(\varepsilon_2-\varepsilon_3)^2+(\varepsilon_3-\varepsilon_1)^2]\right)^{\frac{1}{2}}$$

Where:

v' = effective Poisson' ratio.

Equivalent (von mises) stress, σ_e is related to principle stress by the equation:

$$\sigma_e = \left(\frac{1}{2}[(\sigma_1-\sigma_2)^2+(\sigma_2-\sigma_3)^2+(\sigma_3-\sigma_1)^2]\right)^{\frac{1}{2}}$$

Von mises stress was used in the study because it allows any arbiter three-dimensional stress state to be represented as a single positive stress value.

STRUCTURAL PROBES – The following probes were applied to corrosion area in order to check for localised solution/result.

Table 5: Structural probes.

Probe type	Output	Characteristic
Deformation	Deformation in total	Scope to: Pitting corrosion surface
Strain	Equivalent (von-mises)	
Stress	Equivalent (von-mises)	

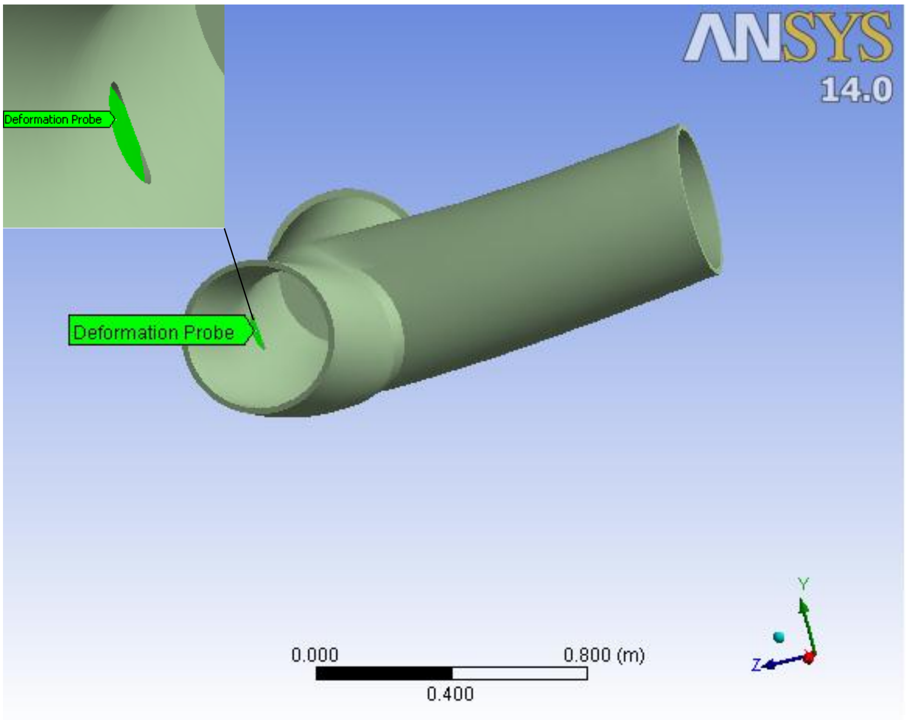

Figure 15: Deformation probe at corrosion area in pipe bend

Fig. 15 shows the location of probe in pipe bend which is the surface of pitting corrosion. For other models, the probes were place in accordance to the corrosion location respectively.

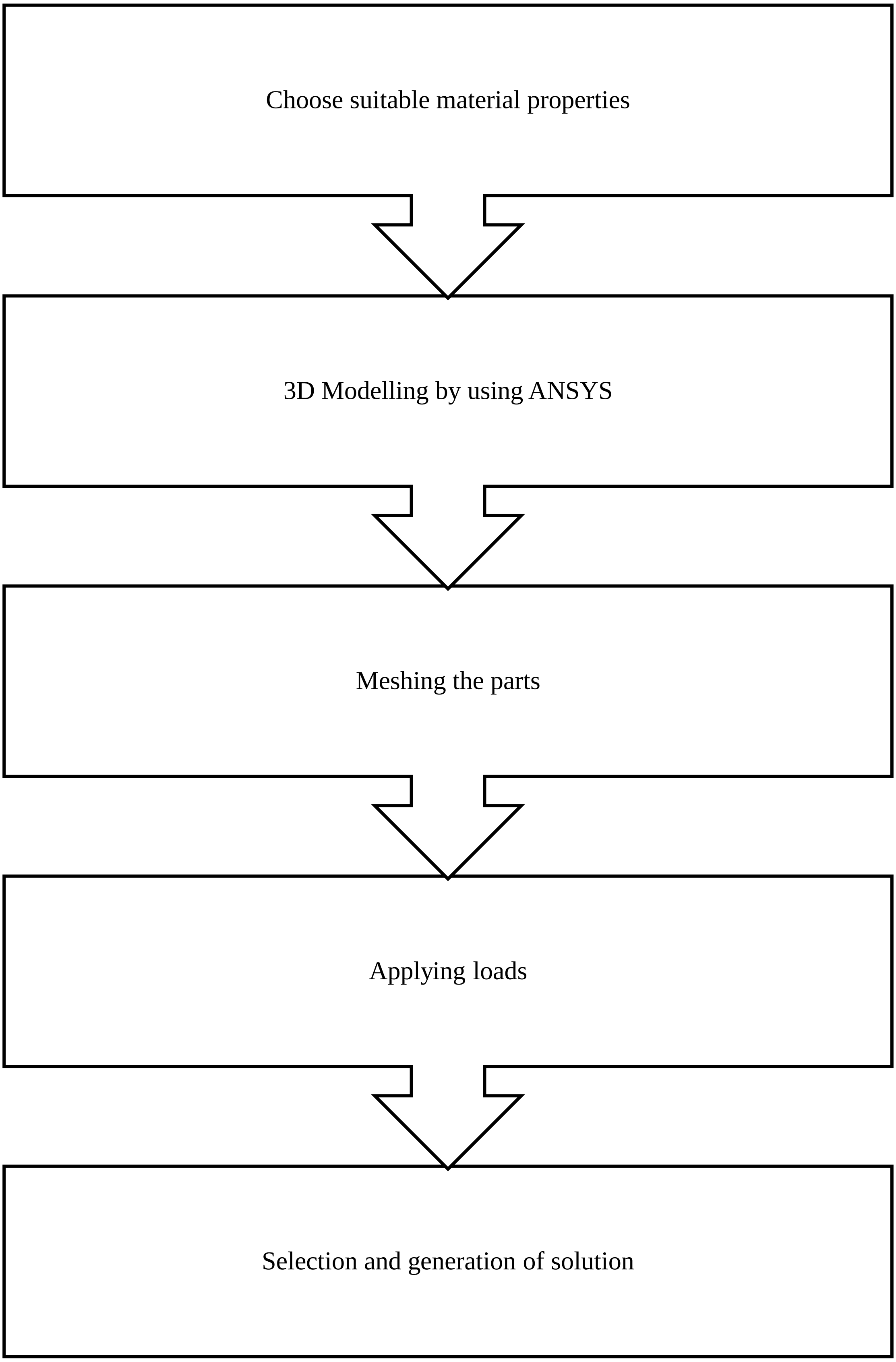

Figure 16: Stages for modelling a corroded pipeline.

3.3. Research Methodology

Referring to fig 11, this research was conducted based on the following planned activities towards the completion of FYP 1 and FYP 2:

1. Research and Literature Review.

   The aim of literature review is to provide better understanding on the terms, keywords on previous conducted research. Not only that, it is to describe and minimize scope of problem before start of a research. Literature review is carried out by reading and cross referencing to any journal articles, books, online resources and other source of researches to obtain related issues to the project carried on.

2. Proposal writing

   The objectives and problem statement are stated clearly on the proposal. The scope of study must be relevant and feasible with the available duration and must be deliverable.

3. Experimental design

   Gathering data and information for this project is done from studies and calculations to come up with the most effective model. During simulation, a suitable loading or pressure will be applied to the model.

4. Simulation testing

   Simulation for pipeline bend will be carried out by ANSYS. ANSYS was selected to be simulating software due to its reliability and user-friendly interface.

5. Model improvement and modification

   Improvement on the design should be done if the preliminary result does not meet the requirements. The process is repeated until satisfactory result is obtained.

6. Result analysis

   The final stage of this research is to analyse the simulation result and will be compared with available industrial codes.

3.4. Project activities

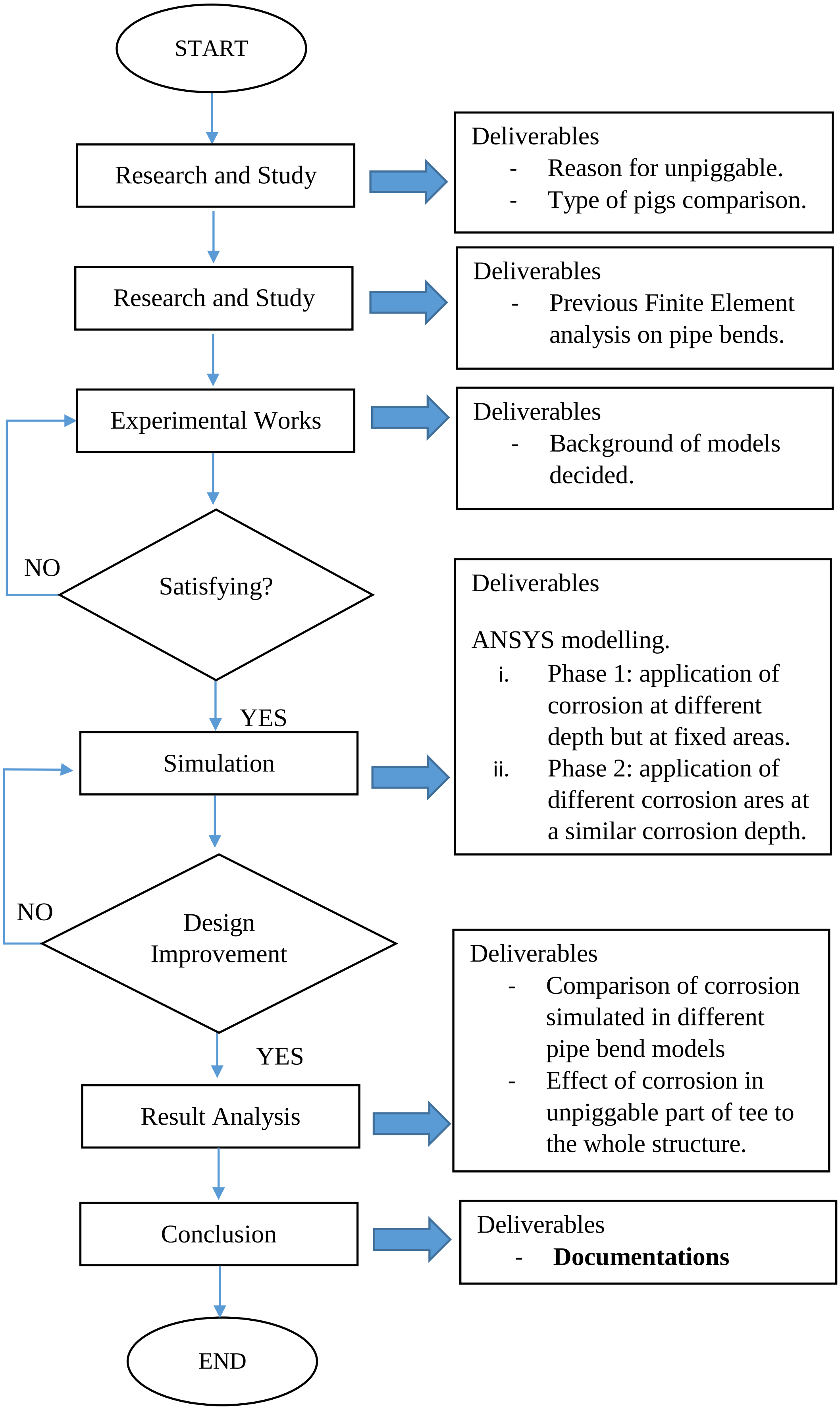

Figure 17: Project activities.

3.5. Key milestone

For FYP 1, during the first semester, the following milestones should be completed during the given time.

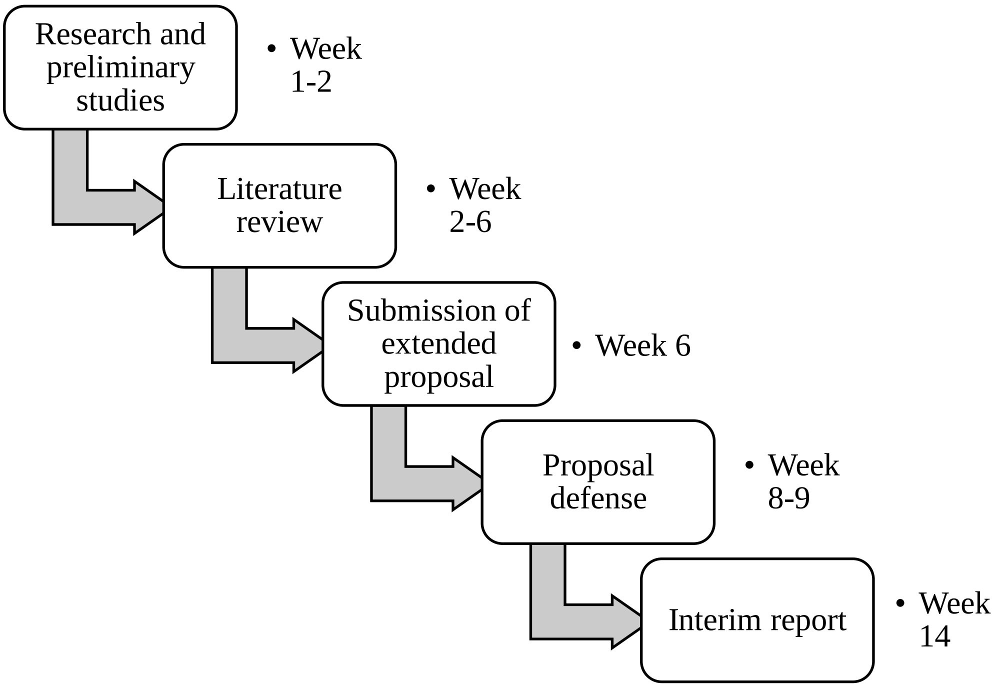

Figure 18: Key milestone for FYP 1.

During FYP 2, the research is more towards practical works rather than planning and topic understanding. The proposed key milestones for FYP 2 are as followed:

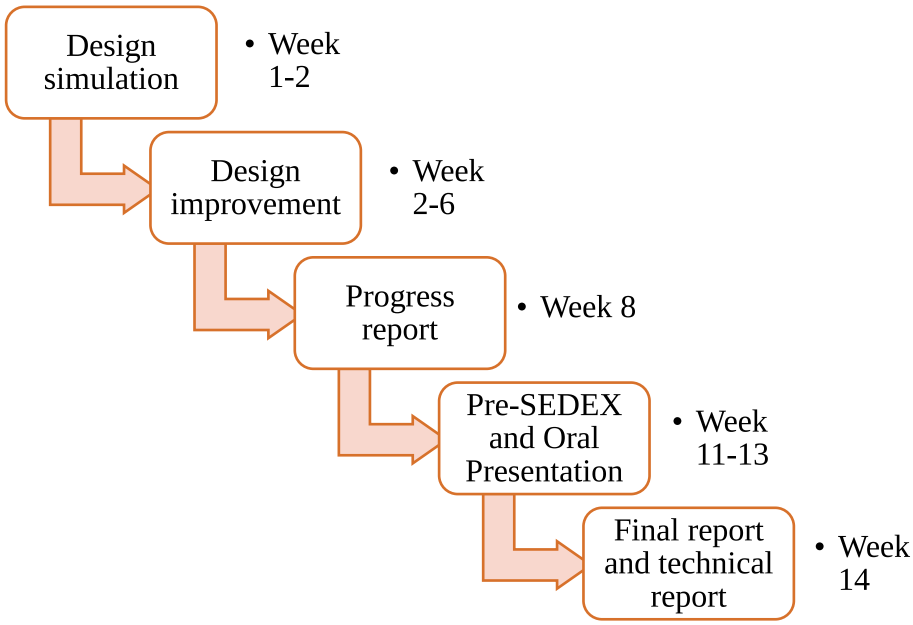

Figure 19: Key milestone for FYP 2

CHAPTER 4

RESULT AND ANALYSIS

4.1. Simulated Standard 90° pipe bend, model #1

4.1.1. ANSYS Mechanical Model

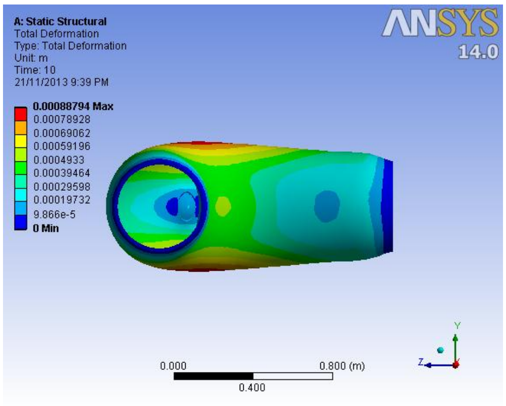

Figure 22: Total deformation on standard pipe bend

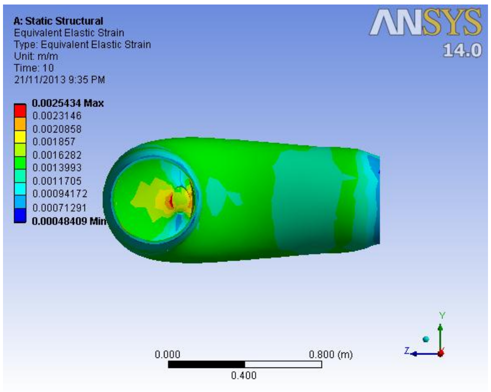

Figure 21: Strain distribution on standard pipe bend

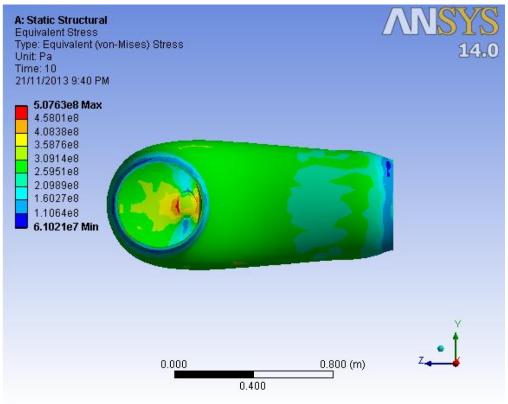

Figure 20: Stress distribution on standard pipe bend

4.1.2. Variation of pitting corrosion depth

a. Data

Table 6 : Total structural solution due to variation of corrosion depth

No	Depth (mm)	Diameter (mm)	Area (mm^2)	Volume (mm^3)	Total		
					Deformation (m)	Strain	Stress (Pa)
1	0	20	314.29	0	8.15E-04	2.22E-03	4.44E+08
2	1	20	314.29	314.2857	7.90E-04	2.12E-03	4.23E+08
3	2	20	314.29	628.5714	7.99E-04	2.10E-03	4.19E+08
4	3	20	314.29	942.8571	7.95E-04	2.10E-03	4.19E+08
5	4	20	314.29	1257.143	7.99E-04	2.33E-03	4.66E+08
6	5	20	314.29	1571.429	8.03E-04	2.10E-03	4.19E+08
7	6	20	314.29	1885.714	7.94E-04	2.53E-03	4.95E+08
8	7	20	314.29	2200	7.98E-04	2.44E-03	4.83E+08
9	8	20	314.29	2514.286	7.92E-04	2.57E-03	5.08E+08
10	9	20	314.29	2828.571	7.94E-04	2.78E-03	5.47E+08
11	10	20	314.29	3142.857	7.94E-04	2.77E-03	5.48E+08
12	11	20	314.29	3457.143	7.92E-04	2.57E-03	5.08E+08

Table 7 : Structural probe solution due to variation of corrosion depth

No	Depth (mm)	Diameter (mm)	Area (mm^2)	Volume (mm^3)	Probe		
					Deformation (m)	Strain	Stress (Pa)
1	0	20	314.29	0			
2	1	20	314.29	314.2857	3.80E-04	1.44E-03	2.88E+08
3	2	20	314.29	628.5714	3.78E-04	1.70E-03	3.31E+08
4	3	20	314.29	942.8571	3.75E-04	1.82E-03	3.42E+08
5	4	20	314.29	1257.143	3.74E-04	1.88E-03	3.66E+08
6	5	20	314.29	1571.429	3.77E-04	1.67E-03	3.11E+08
7	6	20	314.29	1885.714	3.68E-04	1.80E-03	3.50E+08
8	7	20	314.29	2200	3.72E-04	1.71E-03	3.33E+08
9	8	20	314.29	2514.286	3.65E-04	1.77E-03	3.47E+08
10	9	20	314.29	2828.571	3.68E-04	1.69E-03	3.26E+08
11	10	20	314.29	3142.857	3.67E-04	1.75E-03	3.38E+08
12	11	20	314.29	3457.143	3.67E-04	1.60E-03	3.10E+08

b. Comparison Graph

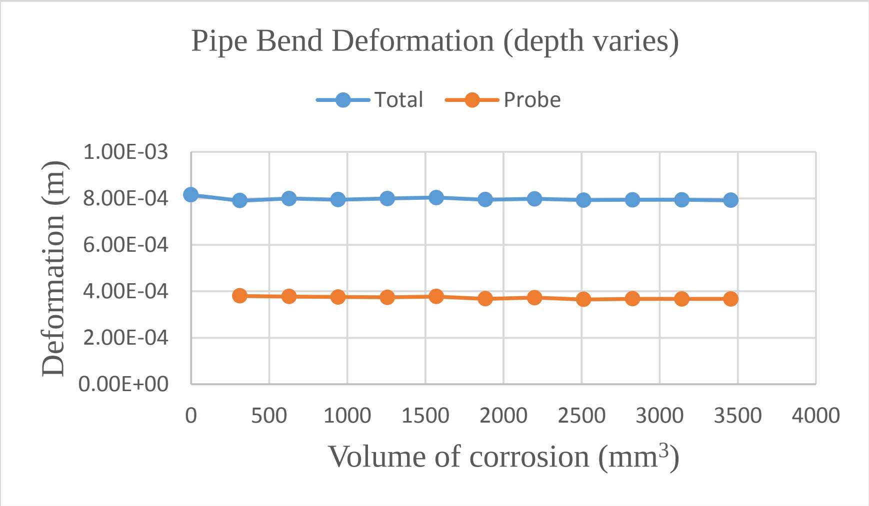

Figure 23: Graph of pipe bend deformation (depth varies)

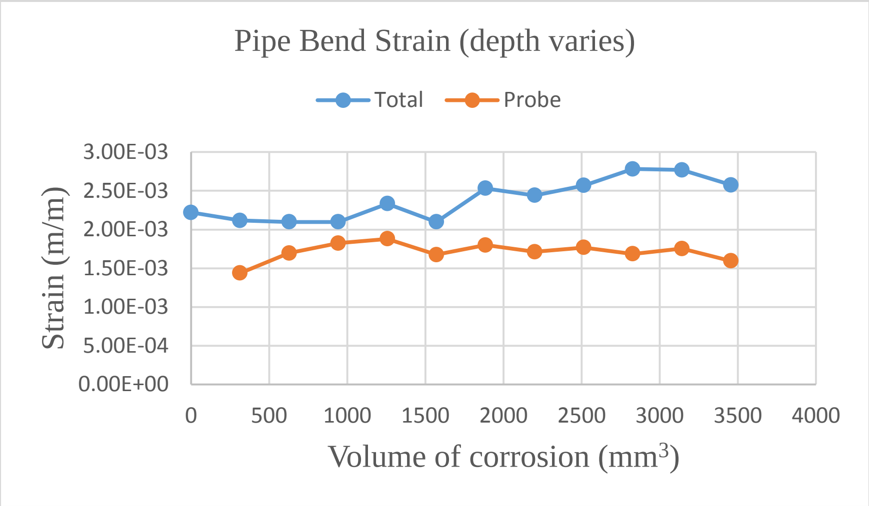

Figure 24: Graph of pipe bend strain (depth varies)

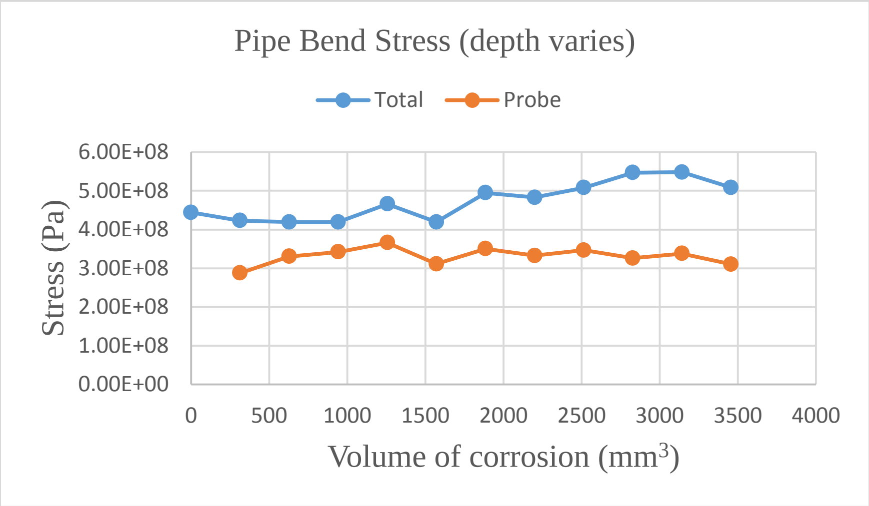

Figure 25: Graph of pipe bend stress (depth varies)

4.1.3. Variation of pitting corrosion area

a. Data

Table 8 : Total structural solution due to variation of corrosion area

No	Depth (mm)	Diameter (mm)	Area (mm^2)	Volume (mm^3)	Total		
					Deformation (m)	Strain	Stress (Pa)
1	1	0	0.00	0	8.15E-04	2.22E-03	4.44E+08
2	1	10	78.57	78.5714	7.96E-04	2.07E-03	4.14E+08
3	1	20	314.29	314.286	8.00E-04	2.12E-03	4.23E+08
4	1	30	707.14	707.143	8.00E-04	2.11E-03	4.20E+08
5	1	40	1257.14	1257.14	8.05E-04	2.14E-03	4.28E+08
6	1	50	1964.29	1964.29	8.16E-04	2.10E-03	4.19E+08
7	1	60	2828.57	2828.57	8.07E-04	2.43E-03	4.86E+08
8	1	70	3850.00	3850	8.29E-04	2.21E-03	4.42E+08

Table 9 : Structural probe solution due to variation of corrosion area

No	Depth (mm)	Diameter (mm)	Area (mm^2)	Volume (mm^3)	Probe		
					Deformation (m)	Strain	Stress (Pa)
1	1	0	0.00	0			
2	1	10	78.57	78.5714	3.99E-04	1.59E-03	3.09E+08
3	1	20	314.29	314.286	3.81E-04	1.46E-03	2.91E+08
4	1	30	707.14	707.143	3.53E-04	1.70E-03	3.37E+08
5	1	40	1257.14	1257.14	3.23E-04	1.78E-03	3.44E+08
6	1	50	1964.29	1964.29	2.74E-04	2.08E-03	4.05E+08
7	1	60	2828.57	2828.57	2.28E-04	2.43E-03	4.86E+08
8	1	70	3850.00	3850	1.78E-04	2.16E-03	4.08E+08

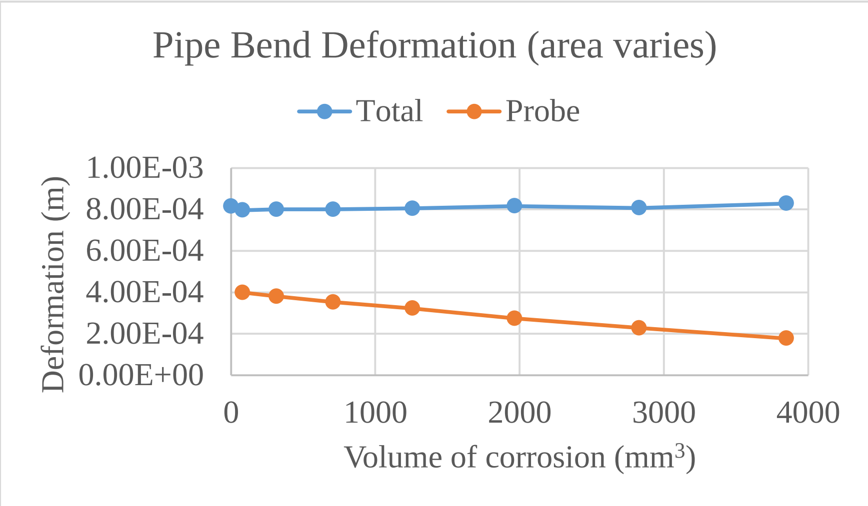

Figure 26: Graph of pipe bend deformation (area varies)

b. Comparison graph

4.1.4. Analysis

a. Total and probe deformation

Fig. 23 shows the pipe bend total and probe deformation graph with increasing corrosion volume. Both data are stabilised with increment of corrosion volume. The pipe model deformation is unaffected by the changes of depth of applied corrosion. Although it appear to change in

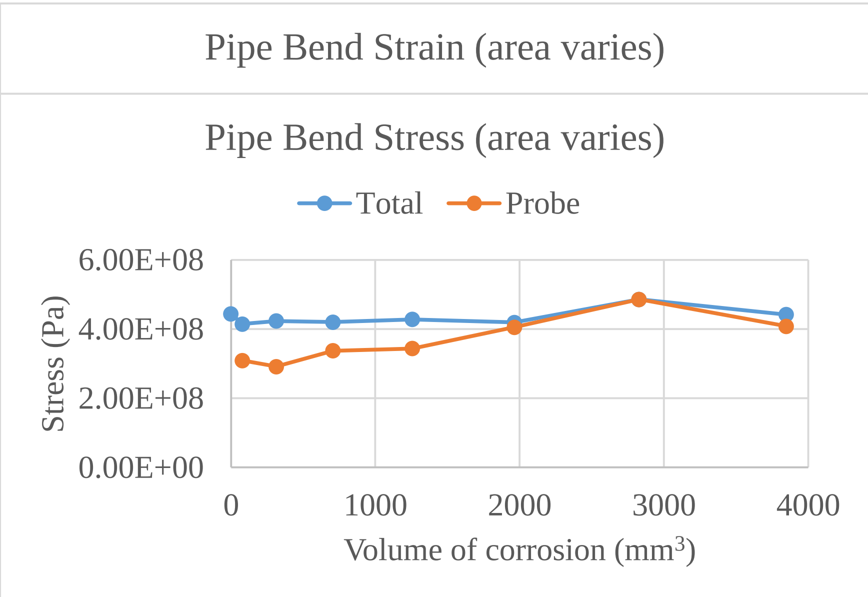

shape, the volume and distortion of material that contribute to deformation is relatively small.

In fig. 26, pipe bend deformation with corrosion surface area variation is demonstrated. The trend for total deformation is similar as depth variation corrosion, but for probe deformation, there is a decreasing in value trend. It means the volume or pipe bend distortion at applied corrosion is relatively high.

b. Total and probe equivalent elastic strain

Fig. 24 indicates the strain in total and structural probe of a pipe bend model when corrosion volume increase by manipulating it depth. Both graph have irregular trends. It can be seen that trends of total strain is differ from probe strain. Corrosion affecting the pipe bend strain but maximum value is at recorded at deferent part from the probe (corrosion surface) due to displacement that affecting strain of the corrosion surface is small.

Meanwhile in fig. 27, strain recorded in pipe bend (total and probe) have a same value when corrosion volume is 2000 mm^3 and above. Corrosion recorded at probe has dominant the total strain.

c. Total and probe equivalent stress.

Stress of pipe bend is illustrated in fig. 25. Key parameter of stress are force and area. Since internal force and area is remain constant, probe stress reading is remain constant. Maximum total stress of pipe bend recorded was 548 MPa.

Fig. 28 indicates the stress recorded after applied corrosion volume 2000 mm^3 also have same values for both total and probe reading. Hence, stress from corrosion surface (probe) governing the failure of the pipe bend model.

4.2. Simulated Miter Bend, model #2

4.2.1. ANSYS Mechanical model

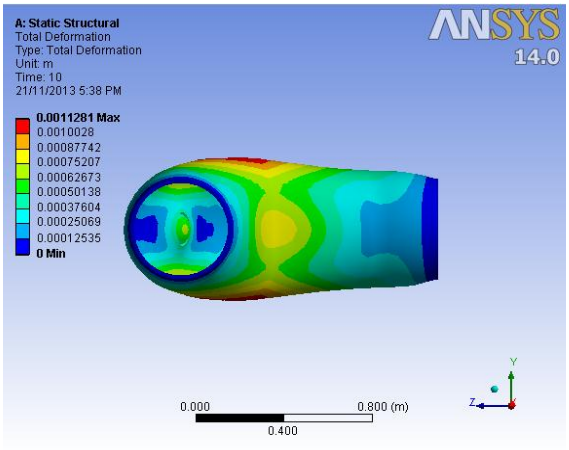

Figure 29: Total deformation of miter bend

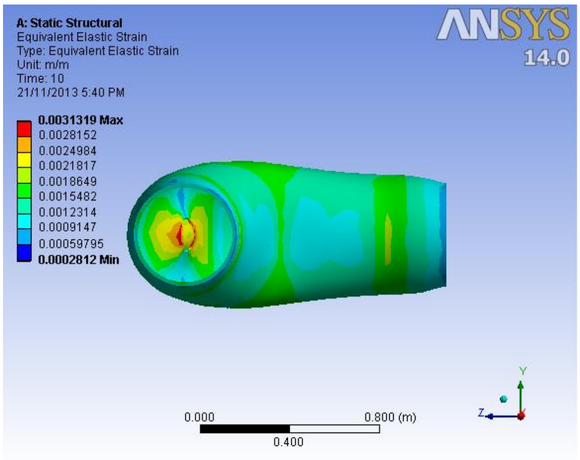

Figure 31: Strain distribution of miter bend

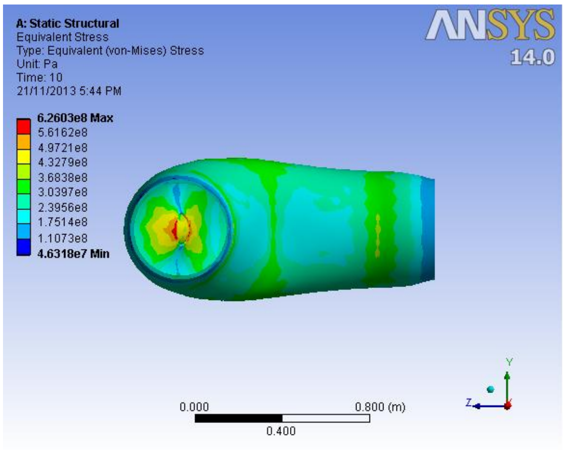

Figure 30: Stress distribution of miter bend

4.2.2. Variation of pitting corrosion depth

a. Data

Table 10 : Total structural solution due to variation of corrosion depth

No	Depth (mm)	Diameter (mm)	Area (mm^2)	Volume (mm^3)	Total		
					Deformation (m)	Strain	Stress (Pa)
1	0	20	314.29	0	1.04E-03	2.80E-03	5.59E+08
2	1	20	314.29	314.2857	9.74E-04	2.77E-03	5.54E+08
3	2	20	314.29	628.5714	9.75E-04	2.78E-03	5.56E+08
4	3	20	314.29	942.8571	9.75E-04	2.78E-03	5.56E+08
5	4	20	314.29	1257.143	9.75E-04	2.88E-03	5.67E+08
6	5	20	314.29	1571.429	9.73E-04	2.77E-03	5.53E+08
7	6	20	314.29	1885.714	9.74E-04	3.03E-03	5.99E+08
8	7	20	314.29	2200	9.74E-04	3.15E-03	6.21E+08
9	8	20	314.29	2514.286	9.74E-04	3.32E-03	6.55E+08
10	9	20	314.29	2828.571	9.74E-04	3.48E-03	6.83E+08
11	10	20	314.29	3142.857	9.74E-04	3.58E-03	6.97E+08
12	11	20	314.29	3457.143	9.74E-04	3.65E-03	7.10E+08

Table 11 : Structural probe solution due to variation of corrosion depth

No	Depth (mm)	Diameter (mm)	Area (mm^2)	Volume (mm^3)	Probe		
					Deformation (m)	Strain	Stress (Pa)
1	0	20	314.29	0			
2	1	20	314.29	314.2857	3.36E-04	1.98E-03	3.95E+08
3	2	20	314.29	628.5714	3.36E-04	2.13E-03	4.17E+08
4	3	20	314.29	942.8571	3.33E-04	1.93E-03	3.77E+08
5	4	20	314.29	1257.143	3.39E-04	1.97E-03	3.88E+08
6	5	20	314.29	1571.429	3.40E-04	2.02E-03	3.98E+08
7	6	20	314.29	1885.714	3.31E-04	1.99E-03	3.93E+08
8	7	20	314.29	2200	3.30E-04	1.98E-03	3.91E+08
9	8	20	314.29	2514.286	3.30E-04	1.93E-03	3.79E+08
10	9	20	314.29	2828.571	3.29E-04	1.97E-03	3.87E+08
11	10	20	314.29	3142.857	3.28E-04	1.95E-03	3.85E+08
12	11	20	314.29	3457.143	3.28E-04	1.91E-03	3.76E+08

b. Comparison graph

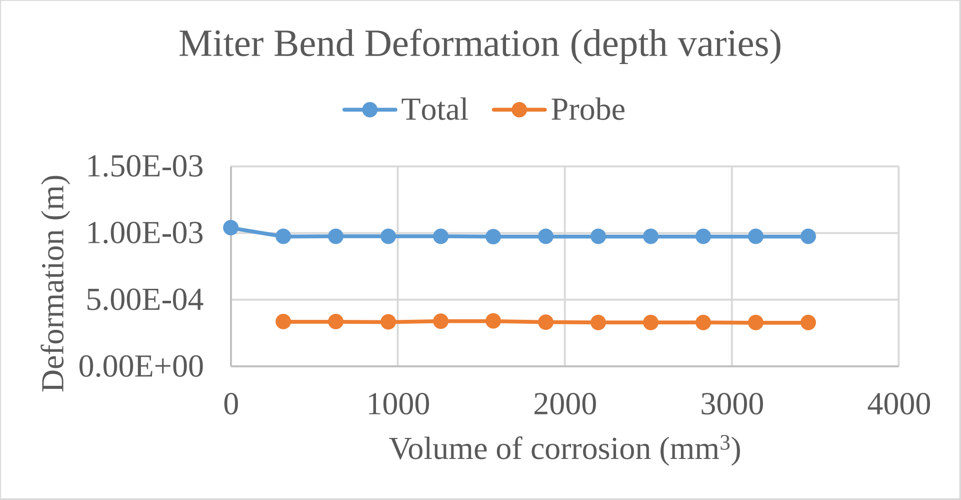

Figure 32: Graph of miter bend deformation (depth varies)

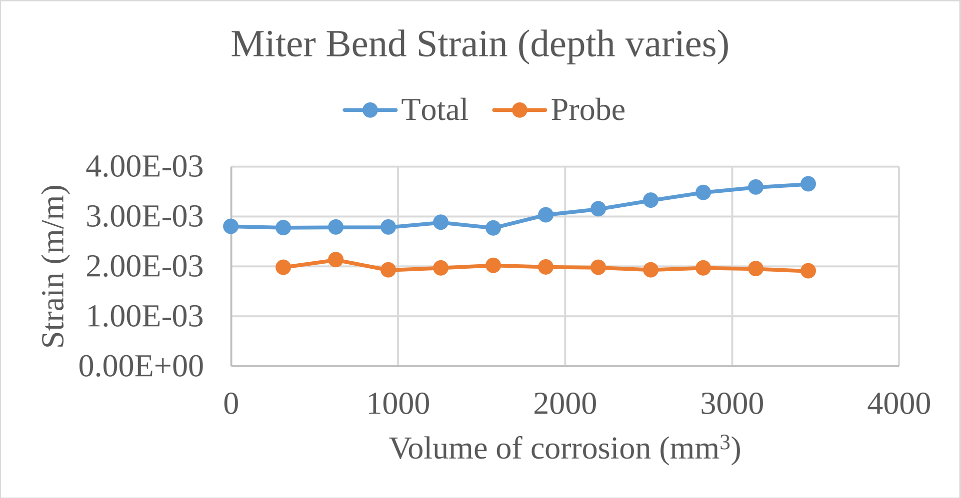

Figure 33: Graph of miter bend strain (depth varies)

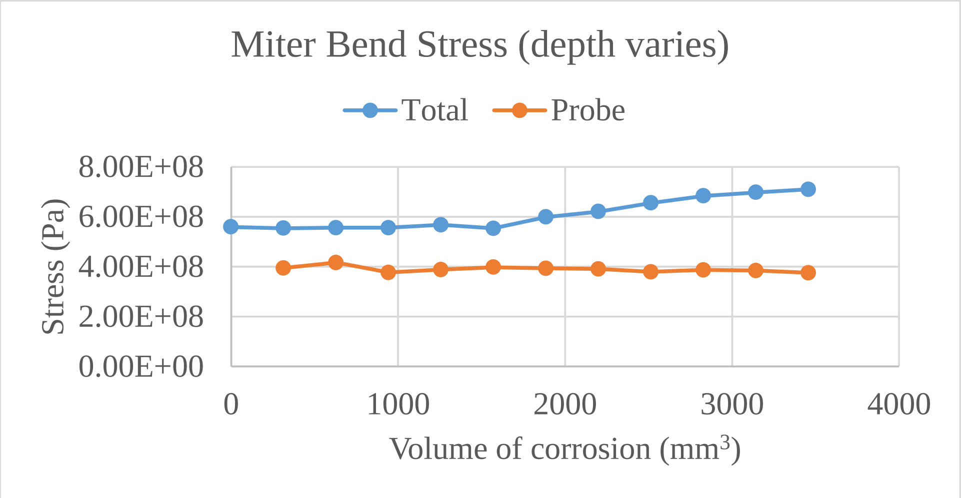

Figure 34: Graph of miter bend stress (depth varies)

4.2.3. Variation of pitting corrosion area.

a. Data

Table 12 : Total structural solution due to variation of corrosion area

No	Depth (mm)	Diameter (mm)	Area (mm^2)	Volume (mm^3)	Total		
					Deformation (m)	Strain	Stress (Pa)
1	1	0	0.00	0	1.04E-03	2.80E-03	5.59E+08
2	1	10	78.57	78.57143	9.70E-04	2.76E-03	5.51E+08
3	1	20	314.29	314.2857	9.74E-04	2.77E-03	5.54E+08
4	1	30	707.14	707.1429	9.78E-04	2.79E-03	5.57E+08
5	1	40	1257.14	1257.143	9.82E-04	2.80E-03	5.59E+08
6	1	50	1964.29	1964.286	1.00E-03	3.07E-03	6.14E+08
7	1	60	2828.57	2828.571	1.01E-03	2.79E-03	5.56E+08
8	1	70	3850.00	3850	1.03E-03	2.80E-03	5.59E+08

Table 13 : Structural probe solution due to variation of corrosion area

No	Depth (mm)	Diameter (mm)	Area (mm^2)	Volume (mm^3)	Probe		
					Deformation (m)	Strain	Stress (Pa)
1	1	0	0.00	0			
2	1	10	78.57	78.57143	3.62E-04	1.73E-03	3.46E+08
3	1	20	314.29	314.2857	3.36E-04	1.98E-03	3.95E+08
4	1	30	707.14	707.1429	3.05E-04	1.85E-03	3.70E+08
5	1	40	1257.14	1257.143	2.50E-04	2.00E-03	4.00E+08
6	1	50	1964.29	1964.286	1.85E-04	3.07E-03	6.14E+08
7	1	60	2828.57	2828.571	9.88E-05	2.62E-03	5.13E+08
8	1	70	3850.00	3850	9.86E-05	2.69E-03	5.21E+08

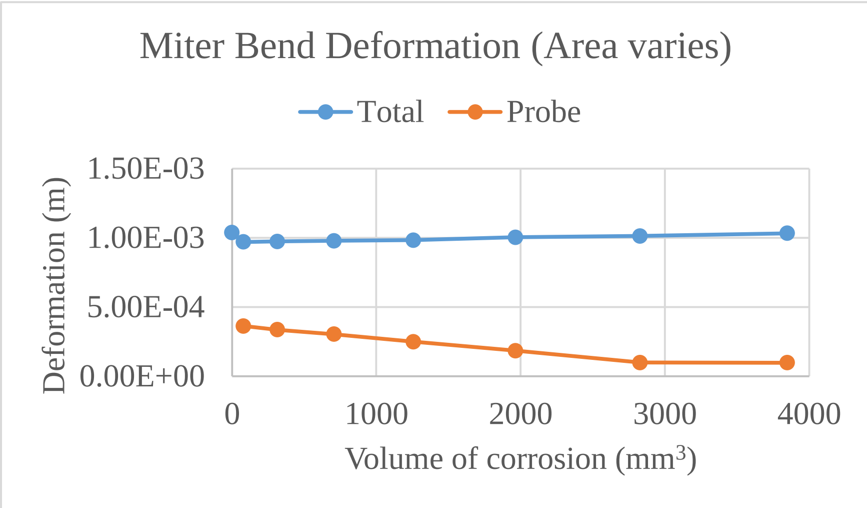

a. Comparison graph

4.2.4. Analysis

a. Total and probe deformation

As shown in fig. 32, miter bend deformation responded similarly as standard pipe bend to an increment of corrosion volume with depth variation. Both total and probe reading remain constant throughout the depth increment. This concluded that changes in corrosion depth will not affecting miter bend deformation.

Figure 36: Graph of miter bend deformation (area varies)

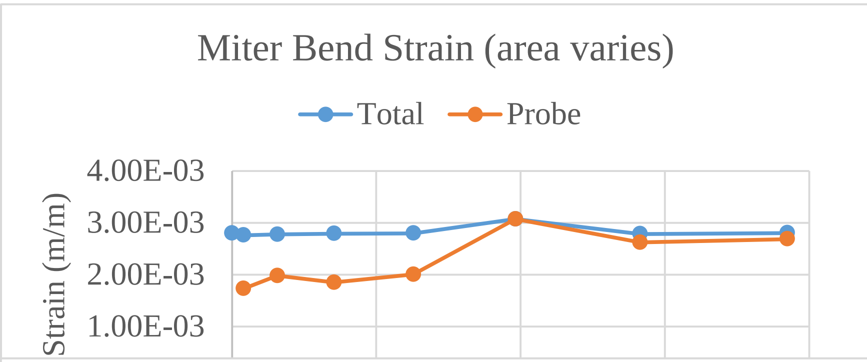

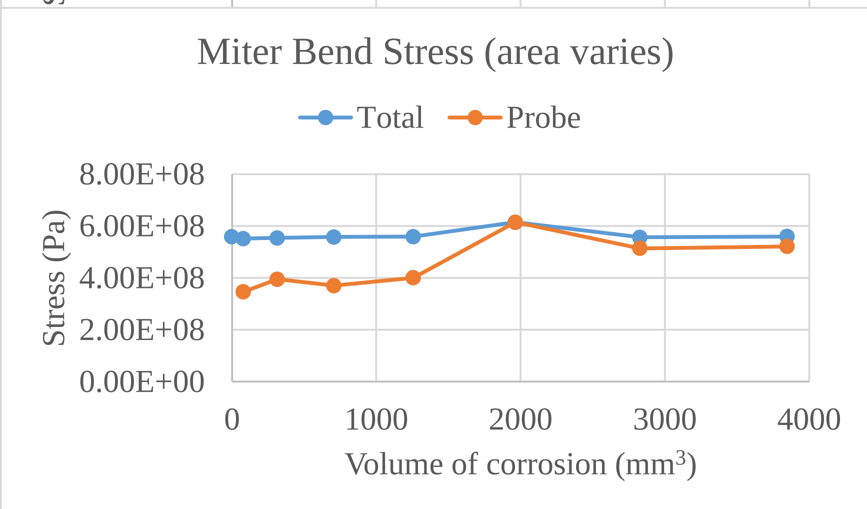

Though total deformation in miter bend strain remains, the probe deformation reading in area variation of corrosion volume shows some gradual decreasing in its deformation. This is due to the deformation at the corrosion surface area is reducing.

b. Total and probe equivalent elastic strain

From fig. 33, the total miter bend strain remain constant until the depth of corrosion changed to 6mm. When the corrosion depth increased, the corrosion started to be affective to the strain. However, probe reading shows that no strain changes in miter bend once the corrosion applied.

When corrosion area set to 1964.29 mm^2, both total and probe strain reading in fig. 36 have the same value. The situation means that probe reading has dictated the total strain measurement. From the value afterward, the trend remains.

c. Total and probe equivalent stress.

Fig. 34 and fig. 37 indicate the stress distribution in miter bend model. At depth 6mm corrosion, the stress distribution in the model has increased gradually. It is resulted from the corrosion depth increment. But, differ in probe reading, it recorded the same stress distribution regardless of depth of corrosion changing. No significant effect from corrosion.

Changing the surface area of corrosion resulted in significant impact to the miter bend model stress distribution. When area increased to 1964.29mm, the stress distribution in total structure depend on on probe stress distribution. It is indicating the corrosion area is the part where stress is at maximum level and has become a stress limiting factor.

4.3. Simulated unbarred full-bored pipe bend near dead end (Tee), model #3

4.3.1. ANSYS Mechanical model

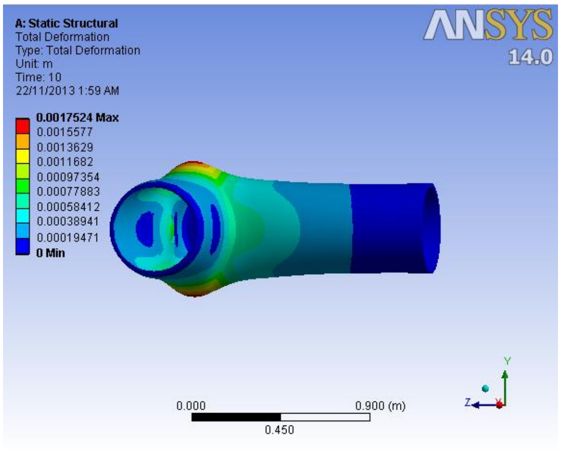

Figure 38: Total deformation in tee model.

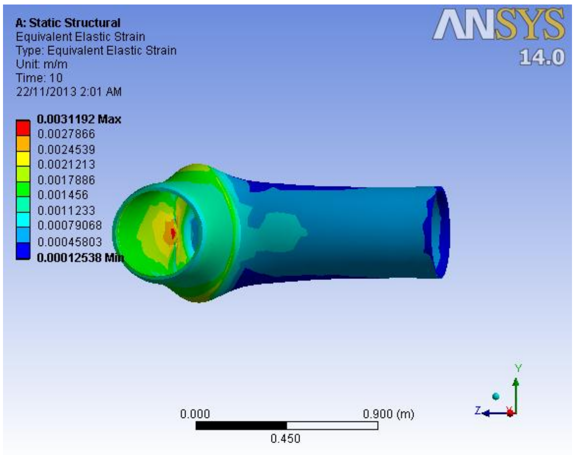

Figure 39: Strain distribution in tee model.

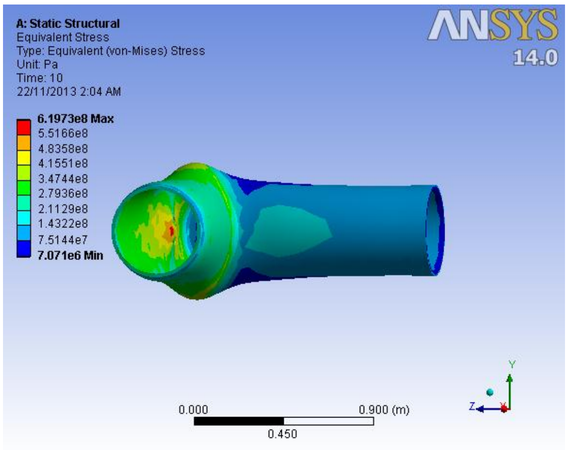

Figure 40: Stress distribution in tee model.

4.3.2. Variation of pitting corrosion depth

a. Data

Table 14 : Total structural solution due to variation of corrosion depth

No	Depth (mm)	Diameter (mm)	Area (mm^2)	Volume (mm^3)	Total		
					Deformation (m)	Strain	Stress (Pa)
1	0	20	314.29	0	1.51E-03	2.65E-03	5.24E+08
2	1	20	314.29	314.2857	1.51E-03	2.77E-03	5.51E+08
3	2	20	314.29	628.5714	1.52E-03	2.96E-03	5.91E+08
4	3	20	314.29	942.8571	1.50E-03	2.86E-03	5.68E+08
5	4	20	314.29	1257.143	1.48E-03	2.97E-03	5.82E+08
6	5	20	314.29	1571.429	1.50E-03	3.44E-03	6.82E+08
7	6	20	314.29	1885.714	1.49E-03	3.53E-03	7.00E+08
8	7	20	314.29	2200	1.50E-03	3.71E-03	7.35E+08
9	8	20	314.29	2514.286	1.49E-03	3.76E-03	7.43E+08
10	9	20	314.29	2828.571	1.50E-03	3.88E-03	7.67E+08
11	10	20	314.29	3142.857	1.49E-03	3.77E-03	7.44E+08
12	11	20	314.29	3457.143	1.50E-03	3.99E-03	7.88E+08

Table 15 : Structural probe solution due to variation of corrosion depth

No	Depth (mm)	Diameter (mm)	Area (mm^2)	Volume (mm^3)	Probe		
					Deformation (m)	Strain	Stress (Pa)
1	0	20	314.29	0			
2	1	20	314.29	314.2857	8.15E-05	2.05E-03	4.10E+08
3	2	20	314.29	628.5714	7.92E-05	2.54E-03	4.91E+08
4	3	20	314.29	942.8571	6.30E-05	2.31E-03	4.60E+08
5	4	20	314.29	1257.143	3.27E-05	2.16E-03	4.29E+08
6	5	20	314.29	1571.429	6.75E-05	2.14E-03	4.25E+08
7	6	20	314.29	1885.714	4.93E-05	2.05E-03	4.07E+08
8	7	20	314.29	2200	6.85E-05	2.04E-03	4.06E+08
9	8	20	314.29	2514.286	5.05E-05	1.98E-03	3.93E+08
10	9	20	314.29	2828.571	6.75E-05	1.87E-03	3.73E+08
11	10	20	314.29	3142.857	4.89E-05	1.96E-03	3.87E+08
12	11	20	314.29	3457.143	6.85E-05	1.71E-03	3.39E+08

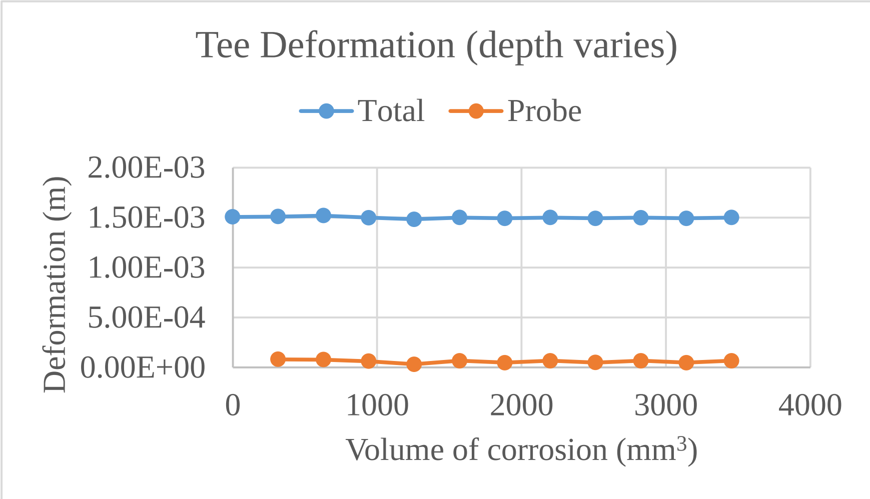

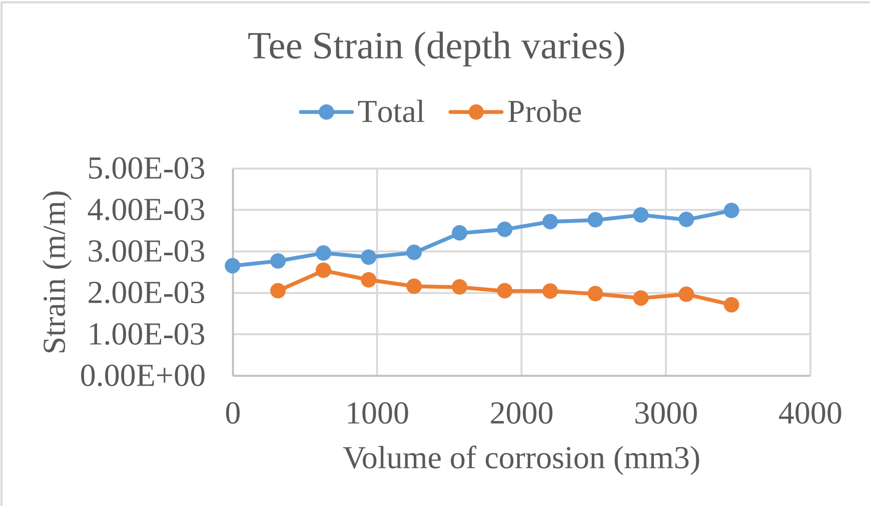

Figure 41: Graph of tee strain (depth varies)

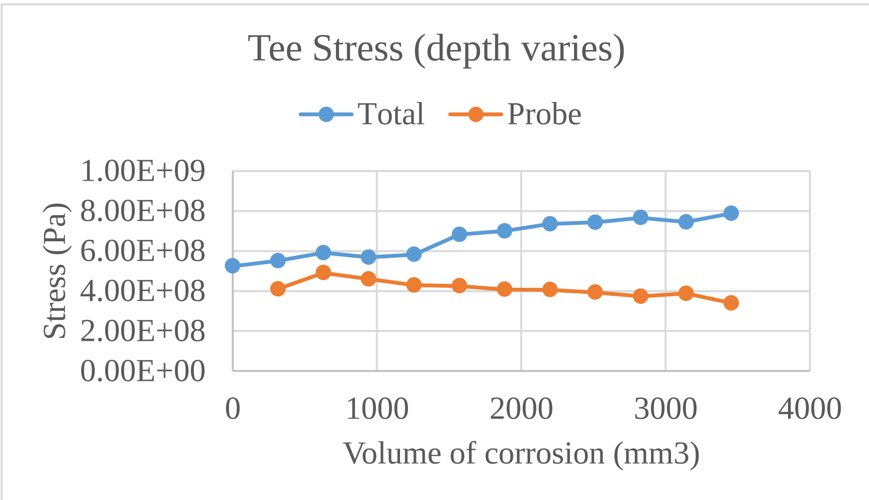

b. Comparison graph

4.3.3. Variation of pitting corrosion area

a. Data

Table 16 : Total structural solution due to variation of corrosion area

No	Depth (mm)	Diameter (mm)	Area (mm^2)	Volume (mm^3)	Total		
					Deformation (m)	Strain	Stress (Pa)
1	1	0	0.00	0	1.04E-03	2.80E-03	5.59E+08
2	1	10	78.57	78.57143	9.70E-04	2.76E-03	5.51E+08
3	1	20	314.29	314.2857	9.74E-04	2.77E-03	5.54E+08
4	1	30	707.14	707.1429	9.78E-04	2.79E-03	5.57E+08
5	1	40	1257.14	1257.143	9.82E-04	2.80E-03	5.59E+08
6	1	50	1964.29	1964.286	1.00E-03	3.07E-03	6.14E+08
7	1	60	2828.57	2828.571	1.01E-03	2.79E-03	5.56E+08
8	1	70	3850.00	3850	1.03E-03	2.80E-03	5.59E+08

Figure 42: Graph of tee deformation (depth varies)

Table 17 : Structural probe solution due to variation of corrosion area

No	Depth (mm)	Diameter (mm)	Area (mm^2)	Volume (mm^3)	Probe		
					Deformation (m)	Strain	Stress (Pa)
1	1	0	0.00	0			
2	1	10	78.57	78.57143	3.62E-04	1.73E-03	3.46E+08
3	1	20	314.29	314.2857	3.36E-04	1.98E-03	3.95E+08
4	1	30	707.14	707.1429	3.05E-04	1.85E-03	3.70E+08
5	1	40	1257.14	1257.143	2.50E-04	2.00E-03	4.00E+08
6	1	50	1964.29	1964.286	1.85E-04	3.07E-03	6.14E+08
7	1	60	2828.57	2828.571	9.88E-05	2.62E-03	5.13E+08
8	1	70	3850.00	3850	9.86E-05	2.69E-03	5.21E+08

Figure 43: Graph of tee strain (depth varies)

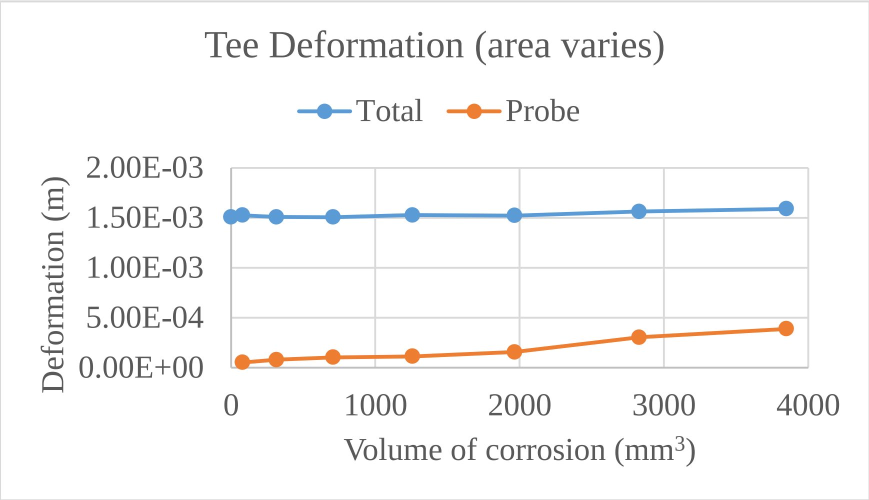

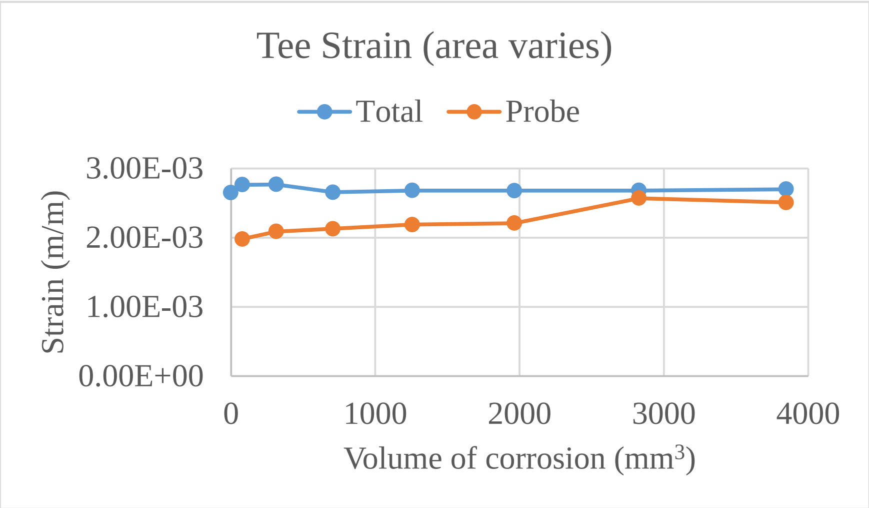

Figure 44: Graph of tee strain (area varies)

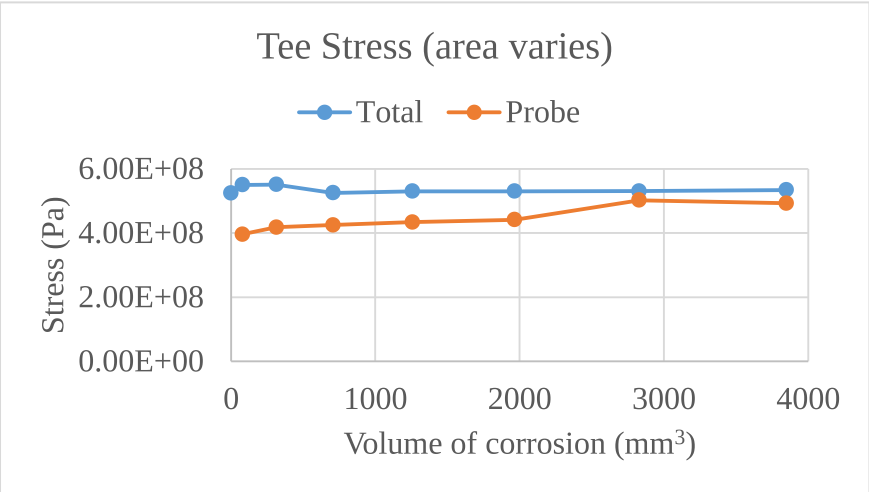

b. Comparison graph

Figure 46: Graph of tee deformation (area varies)

4.3.4. Analysis

a. Total and probe deformation

The pipe deformation remains constant as the depth of corrosion increased. As per fig. 41, both total and probe deformation reading remain unchanged even though the corrosion applied has been increased. Corrosion has no effect to the model when its depth is altered.

From fig. 44, both data of tee deformation represent increment in value due to increment of corrosion area. Corrosion depth increment resulting this changes as its changes proportionally the deformation of localised and total structure deformation.

b. Total and probe equivalent elastic strain

In fig. 42, the total strain keep increasing meanwhile the probe reading shows the decreasing value of elastic strain of the model. The strain is increased at other part of the model. This is an indicator that any changes in corrosion depth will not directly affecting the area where the corrosion applied. It is due to geometrical reason.

For manipulated corrosion area, the total stress has a constant trend. At area of 2828.57 mm^2 the probe reading begin to influencing the total strain of the model. It indicates the corrosion has affecting the total strain after the applied area of corrosion.

c. Total and probe equivalent stress.

Equivalent stress is directly related to area. When area was kept constant as shown in fig. 43, the stress distribute differently from total and probe reading. Total stress is increasing but probe stress reading is decreasing. It can be determined that with the applied corrosion depth, it is not sufficient to influence the total stress distribution.

As area is used as manipulative variable, the graph plotted differently. Total stress distribution remains, while probe reading data is approaching the value of total stress. It started to stimulate the total stress value.

4.4. Simulated unbarred full bore pipe bend near dead end with additional corrosion at difficult area, model #4

4.4.1. ANSYS Mechanical model

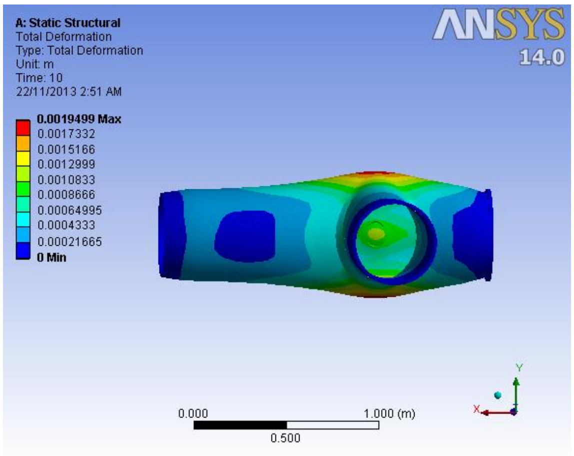

Figure 47: Total deformation at model #4

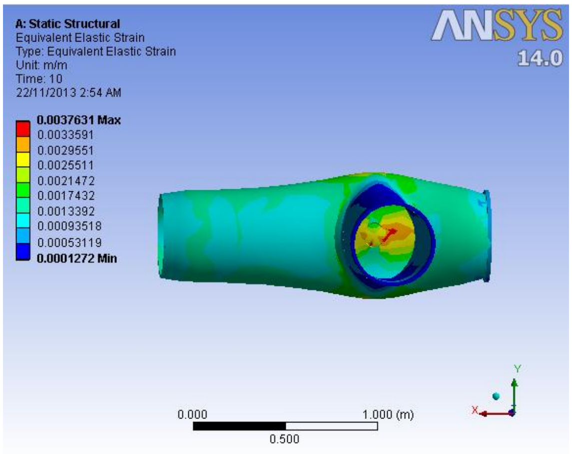

Figure 49: Stress distribution at model #4

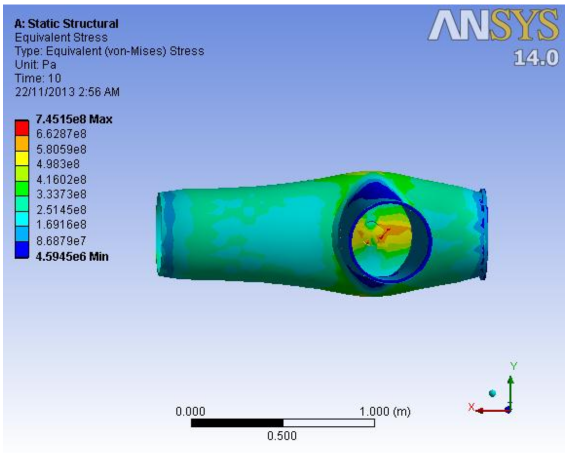

Figure 48: Stress distribution at model #4

4.4.2. Variation of pitting corrosion depth

a. Data

Table 18 : Total structural solution due to variation of corrosion depth

No	Depth (mm)	Diameter (mm)	Area (mm^2)	Volume (mm^3)	Total		
					Deformation (m)	Strain	Stress (Pa)
1	0	20	314.29	0	1.51E-03	2.65E-03	5.24E+08
2	1	20	314.29	314.2857	1.51E-03	2.66E-03	5.27E+08
3	2	20	314.29	628.5714	1.54E-03	2.92E-03	5.80E+08
4	3	20	314.29	942.8571	1.57E-03	3.01E-03	5.99E+08
5	4	20	314.29	1257.143	1.54E-03	3.36E-03	6.52E+08
6	5	20	314.29	1571.429	1.54E-03	3.59E-03	7.09E+08
7	6	20	314.29	1885.714	1.54E-03	3.72E-03	7.35E+08
8	7	20	314.29	2200	1.54E-03	3.88E-03	7.58E+08
9	8	20	314.29	2514.286	1.54E-03	4.03E-03	7.96E+08
10	9	20	314.29	2828.571	1.54E-03	4.18E-03	8.25E+08
11	10	20	314.29	3142.857	1.54E-03	4.10E-03	8.11E+08
12	11	20	314.29	3457.143	1.54E-03	4.27E-03	8.42E+08

Table 19 : Structural probe solution due to variation of corrosion depth

No	Depth (mm)	Diameter (mm)	Area (mm^2)	Volume (mm^3)	Probe		
					Deformation (m)	Strain	Stress (Pa)
1	0	20	314.29	0			
2	1	20	314.29	314.2857	6.59E-05	2.06E-03	4.11E+08
3	2	20	314.29	628.5714	7.06E-05	2.37E-03	4.67E+08
4	3	20	314.29	942.8571	1.23E-04	2.33E-03	4.62E+08
5	4	20	314.29	1257.143	1.24E-04	2.31E-03	4.56E+08
6	5	20	314.29	1571.429	1.31E-04	2.34E-03	4.65E+08
7	6	20	314.29	1885.714	1.32E-04	2.36E-03	4.71E+08
8	7	20	314.29	2200	1.35E-04	2.49E-03	4.89E+08
9	8	20	314.29	2514.286	1.34E-04	1.96E-03	3.88E+08
10	9	20	314.29	2828.571	1.31E-04	2.17E-03	4.32E+08
11	10	20	314.29	3142.857	1.34E-04	1.79E-03	3.55E+08
12	11	20	314.29	3457.143	1.34E-04	1.80E-03	3.50E+08

b. Comparison graph

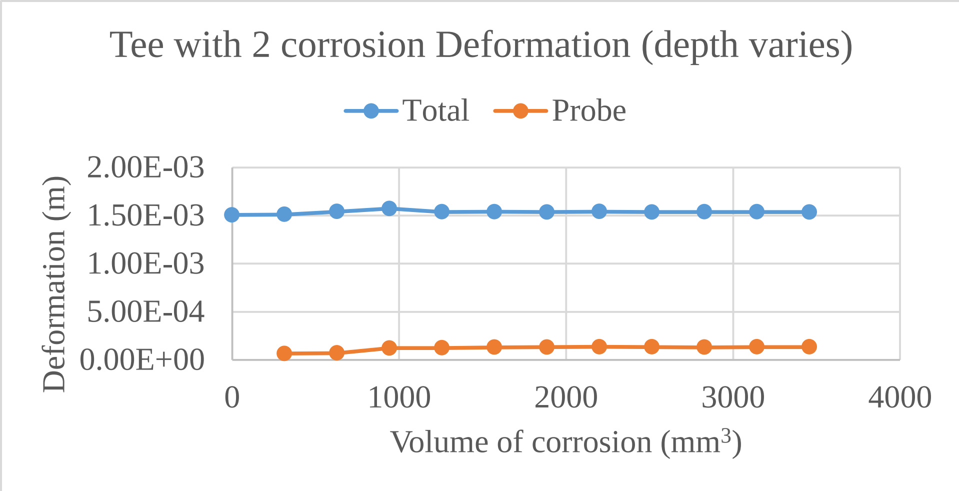

Figure 50: Graph of model #4 deformation (depth varies)

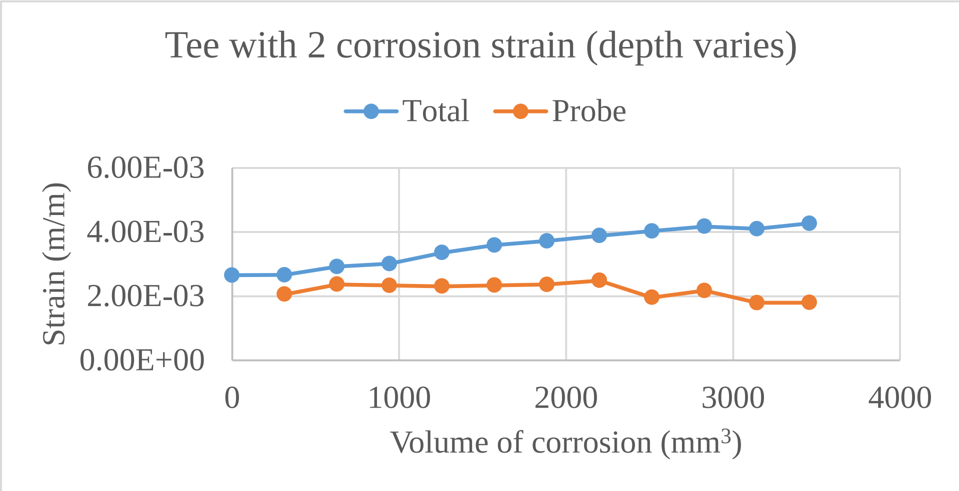

Figure 52: Graph of model #4 strain (depth varies)

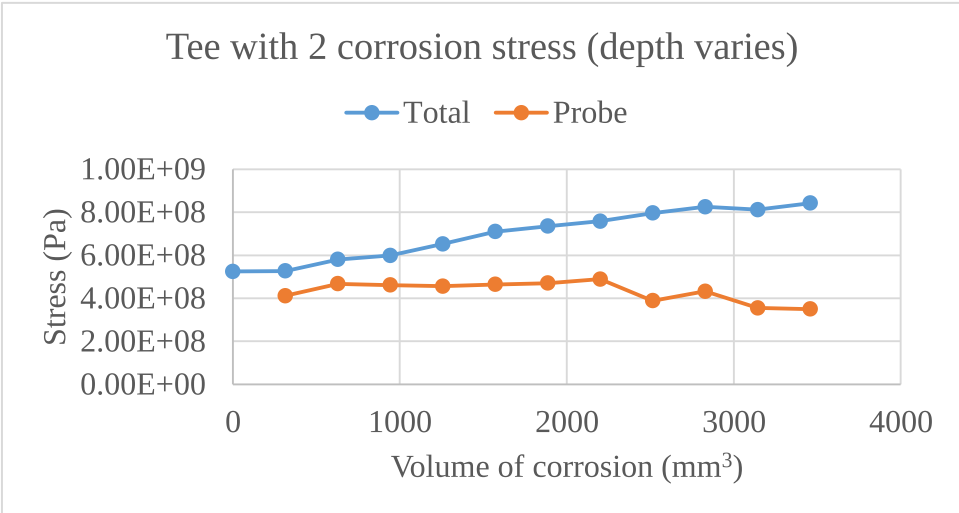

Figure 51: Graph of stress distribution at model #4 (depth varies)

4.4.3. Variation of pitting corrosion area

a. Data

Table 20 : Total structural solution due to variation of corrosion area

No	Depth (mm)	Diameter (mm)	Area (mm^2)	Volume (mm^3)	Total Deformation (m)	Total Strain	Total Stress (Pa)
1	1	0	0.00	0	1.51E-03	2.65E-03	5.24E+08
2	1	10	78.57	78.57143	1.51E-03	2.76E-03	5.50E+08
3	1	20	314.29	314.2857	1.51E-03	2.66E-03	5.27E+08
4	1	30	707.14	707.1429	1.53E-03	2.66E-03	5.27E+08
5	1	40	1257.14	1257.143	1.55E-03	2.68E-03	5.31E+08
6	1	50	1964.29	1964.286	1.59E-03	2.85E-03	5.65E+08
7	1	60	2828.57	2828.571	1.63E-03	2.71E-03	5.41E+08
8	1	70	3850.00	3850	1.68E-03	3.57E-03	7.13E+08

Table 21 : Structural probe solution due to variation of corrosion area

No	Depth (mm)	Diameter (mm)	Area (mm^2)	Volume (mm^3)	Probe Deformation (m)	Probe Strain	Probe Stress (Pa)
1	1	0	0.00	0			
2	1	10	78.57	78.57143	4.71E-05	1.98E-03	3.97E+08
3	1	20	314.29	314.2857	6.20E-05	2.04E-03	4.07E+08
4	1	30	707.14	707.1429	1.41E-04	2.19E-03	4.37E+08
5	1	40	1257.14	1257.143	1.58E-04	2.23E-03	4.40E+08
6	1	50	1964.29	1964.286	2.98E-04	2.85E-03	5.65E+08
7	1	60	2828.57	2828.571	4.17E-04	2.71E-03	5.41E+08
8	1	70	3850.00	3850	6.02E-04	3.57E-03	7.13E+08

b. Comparison graph

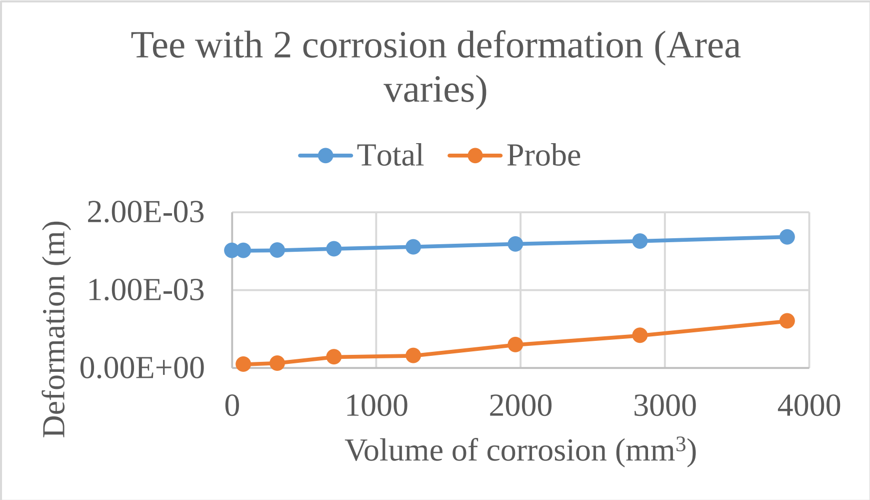

Figure 53: Graph of model #4 stress (area varies)

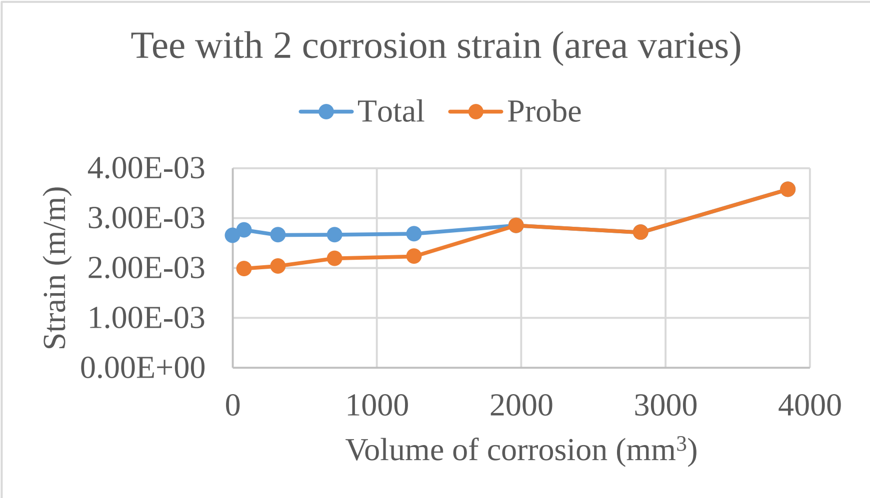

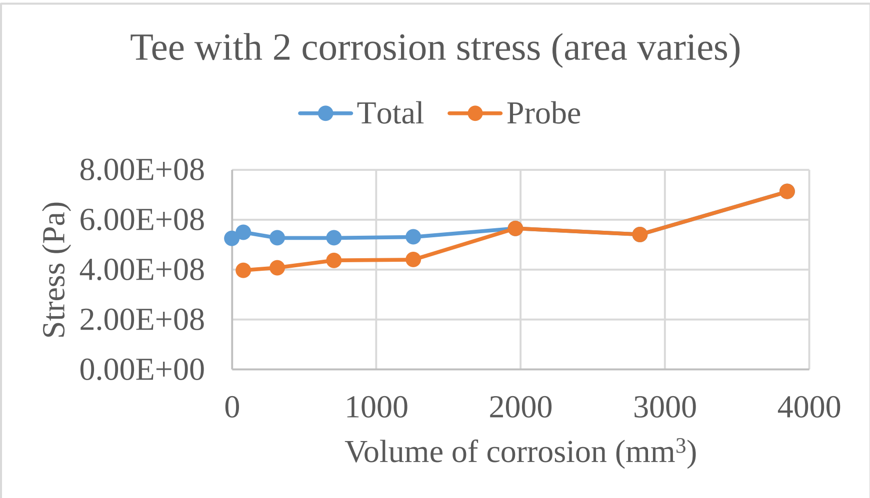

4.4.4. Analysis

a. Total and probe deformation

Fig. 50 denotes the total and probe deformation of pipe tee near dean end with two (2) applied corrosion; middle section and unpiggable portion of the model. Both graphs have stable trends. It remains even with increasing volume of corrosion. With increasing depth only, corrosion applied unpiggable area is not affecting the deformation.

From fig. 53, strain increased in both set of data; total and probe reading. The model finite material deformed from its original form as the corrosion area modified. Thus, corrosion is a limiting factor.

b. Total and probe equivalent elastic strain

Fig. 51 represents strain in total and probe reading. Total equivalent has an increasing trend and probe reading shows irregular sets of data trends. Clearly, corrosion increased the strain in total but not at the probe. Since the probe located at the centre point of middle section corrosion, it unable to read maximum data which occurred in between of the two corrosion.

As shown in fig. 54, at area of 1964.29 mm^2 both graph have same readings. Strain at corrosion applied has become the dominant strain. Its values governing the total strain readings of the model.

Figure 54: Graph of model #4 deformation (area varies)

c. Total and probe equivalent stress.

In fig. 52, stress distribution for total and probe reading are shown. Total stress distribution increase as volume of corrosion increased. But, the probe stress reading remains until area fixed to 2200 mm^2, as it reduced afterwards. Stress distribution increased in total but not manipulating the probe stress reading.

At area of 1964.29 mm^2, stress distribution is affected by the corrosion applied. From that point onward, if the corrosion area increased, the stress distribution will also increase.

Figure 55: Graph of model #4 strain (area varies)

4.5. Summary of analysis

Figure 56 and 57 denote the summary of stress distribution at both parameters.

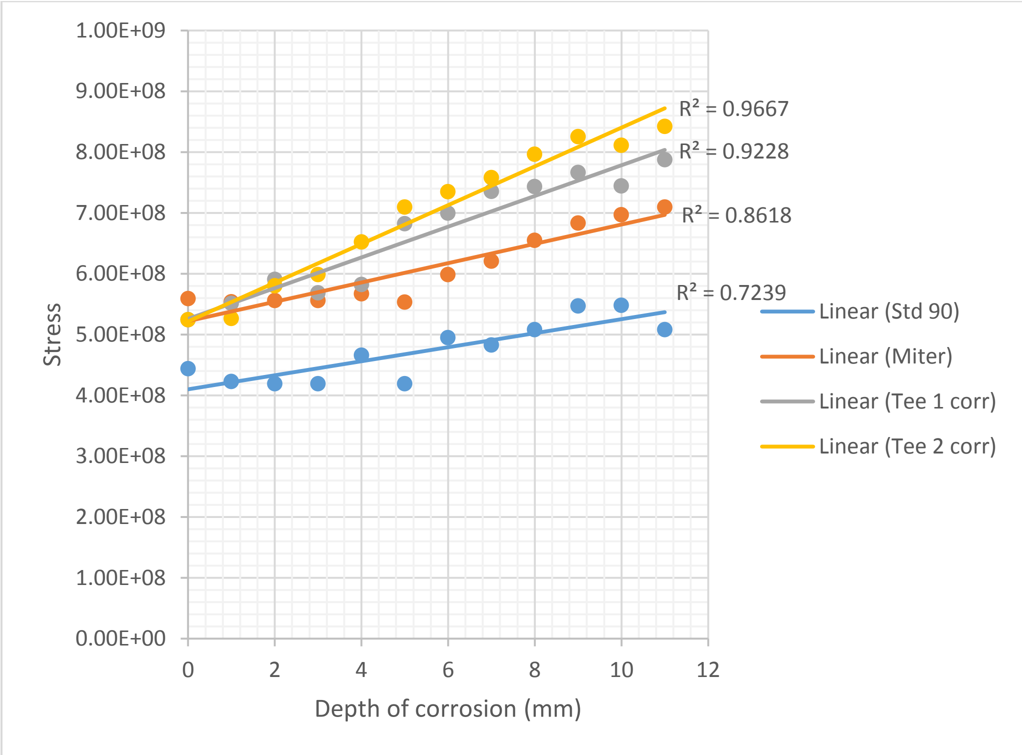

Figure 56: Summary of stress distribution for parameter depth at 4 models.

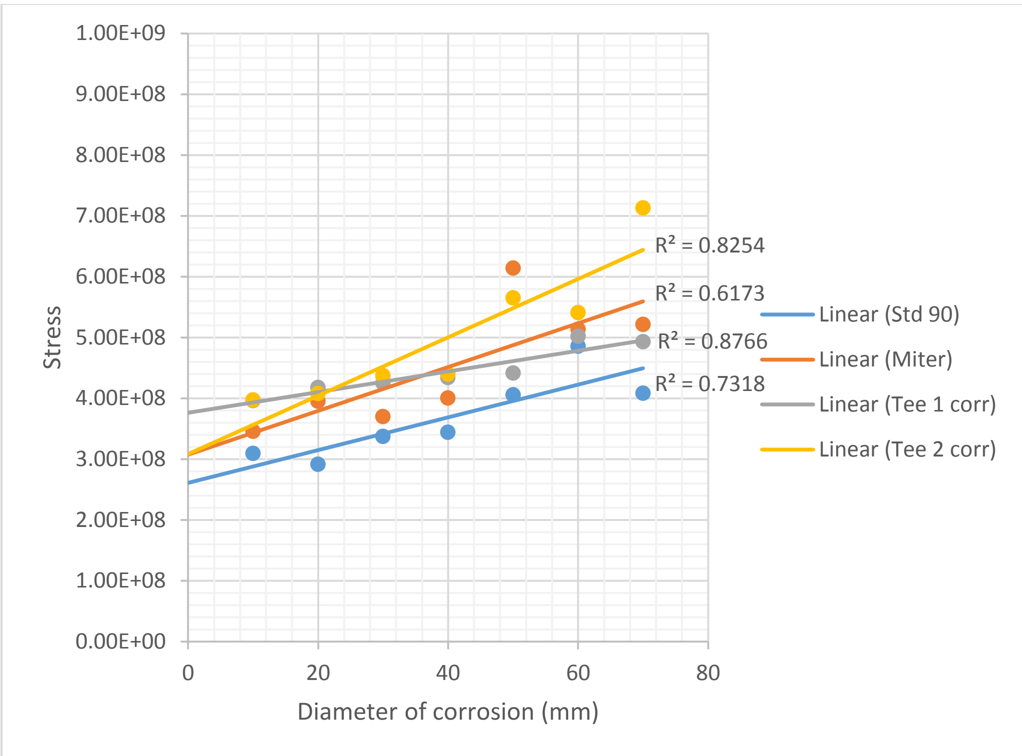

Figure 57: Summary of stress distribution for parameter depth at 4 models.

4.5.1. Discussion

Two parameters of depth and diameter of corrosion were considered in finite element analyses. The value of depth was set to 2.0 mm, 4.0 mm, 6.0 mm, 8.0 mm, 10.0 mm and 12.0 mm. The value of diameter is ranging from 0 to 80 mm were considered. Total of 80 cases were analysed as summarized in fig. 56 and fig. 57.

The results indicate the higher stress observed when the parameter depth was used as variable as compared to diameter. Among the models, unbarred full bore pipe bend near dead end produced highest stress. As expected, model #4 has greater stress compared to model 3. This proves that corrosion at a difficult area will influence the integrity of a pipeline.

CHAPTER 5

CONCLUSION AND RECOMMENDATIONS

5.1. Conclusion

Extensive FEM simulations were presented in this research for pipe bend models with two (2) corrosion parameters. The FEM simulations were to investigate how the depth and diameter of pitting corrosion defects influence the equivalent von mises stress of the defective pipelines.

The results for each models then were compared to examine the effect of geometry to stress distribution of corroded pipelines. Among the models, unbarred full bore pipe bend near dead end produced highest stress with increase in both depth and diameter of corrosion parameters. As predicted, difficult pipe bend with corrosion has greater stress as shown from comparison of model 3 and 4.

The analyses described in the framework of this research investigates the stress distribution of the corroded pipeline models. Corrosion in pipe bend increases the stress at the whole structure. Hence affecting the integrity of the system.

Proper monitoring works required to ensure the corrosion will not damage the pipeline system. It has been shown that the finite element method is well suited for the prediction of pipe bends failure with respect to maximum stress distribution of a pipe bend.

5.2. Suggested future works

a. **Incorporating the geometrical and loading parameter influencing the strength of the pipe bend**; Further research on geometry and loading condition should be consider to ensure the accuracy and precision of the data. Data such as environmental loading, pipe condition under thermal and bending effect need to be included to add practical values of the simulation.

b. **Extension of parameter ranges;** FEM simulation is a reliable tool for inspecting the integrity of the pipeline system. With this advantage, it is best to extend the ranges of parameter for simulation so that the results will have more variation and more critical analysis can be performed.

REFERENCES

About pigs. (n.d). Retrieved from Pipimg Soft: http://www.pipingsoft.com/49/t-1249.html [accessed 6th June 2013]

About Pigs. (n.d). Retrieved from Pigging Production & Services Association: http://www.ppsa-online.com/about-pigs.php [accessed 5th June 2013]

Bhattacharya, A., & Long, D. (2010). A Finite Element-based Investigation on Stress Intensification and Flexibility Factors for Pipe Bend. *NAFEMS Conference.* Oxford: CB&I.

Close Radius Pipe Bending. (2013). Retrieved from Apex Piping: http://www.apexpiping.com/ [accessed 5th June 2013]

Eckart, W., Lietzmann, A., & Rudolp, J. (1996). Linear and nonlinear finite-element analyses of pipe bends. *nternational journal of pressure vessels and piping*, 211-217.

G. Hiltscher, W. M. (2003). *Industrial Pigging Technology.* Freiburg: Wiley-VCH.

Kim, W., Baek, J., & Kim, Y. (2009). integrity Assessment For Corrosion Defect in Hot Bend Pipe of Natural Gas Pipeline. *WGC 2009* (p. 3044). Buenos Aires: International Gas Union.

Krieg, W. (2013). *Practical Solutions for Unpiggable Pipelines – From In-Line Inspection to Robotic Applications.* Retrieved from Rosen Inspection: www.roseninspection.net

Payne, L. (Jan-Mar, 2012). Smart Solution. *Innovation Mag*, pp. 8-10.

Prasad, K. R., & Rao, T. B. (2013). Ovality in Pipe Bends by Finite Element Analysis. *International Journal of Engineering Research and Development*, 91-97.

Roberts, R. (2009). What Do You Know about Pipeline Pigging and Cleaning. *Pipeline & Gas Journal*, 8.

Solid Cast Pigs. (2013). Retrieved from Western Filter Co.: http://www.westernfilterco.com/solid-cast-pigs.php [accessed 7th June 2013]

Steel Mandrels Pig. (2013). Retrieved from Pigs Unlimited International, Inc. [accessed 4th June 2013]

Swart, A., Karamanos, S., Scarpas, A., & Blaauwendraad, J. (2010). Finite element analysis of damage in pipeline bends. *HERON*.

Technical Data. (n.d). Retrieved from Girard Industries: http://www.girardind.com/technical.cfm?cat=1 [accessed 5th June 2013]

Tian Ran Lin, B. G. (2005). *Offshore Pipelines.* Massachusetts: Gulf Professional Publishing.

Wint, D. (n.d.). *Difficult to Pig Pipelines.* Retrieved from TDW Services, Inc: http://www.tdwilliamson.com [accessed 5th June 2013]